

Maximum Agreement Linear Prediction via the Concordance Correlation Coefficient

Taeho Kim¹, George Luta², Matteo Bottai³,
Pierre Chaussé⁴, Gheorghe Doros⁵, and Edsel A. Peña⁶

Abstract

This paper examines distributional properties and predictive performance of the estimated maximum agreement linear predictor (MALP) introduced in Bottai et al. [4], which is the linear predictor maximizing Lin's concordance correlation coefficient (CCC) between the predictor and the predictand. It is compared and contrasted, theoretically and through computer experiments, with the estimated least-squares linear predictor (LSLP). Finite-sample and asymptotic properties are obtained, and confidence intervals are also presented. The predictors are illustrated using two real data sets: an eye data set and a bodyfat data set. The results indicate that the estimated MALP is a viable alternative to the estimated LSLP if one desires a predictor whose predicted values possess higher agreement with the predictand values, as measured by the CCC.

Key Words and Phrases: Asymptotics of Linear Predictors; Concordance Correlation Coefficient; Linear Least-Squares Predictor; Maximum Agreement Linear Predictor; Pearson Correlation Coefficient; Prediction Intervals.

AMS 2020 Subject Classification: Primary: 62J99; Secondary: 62H20, 62F99.

¹Department of Mathematics, Lehigh University. *Email:* tak422@lehigh.edu

²Department of Biostatistics, Bioinformatics & Biomathematics, Georgetown University;
Department of Clinical Epidemiology, Aarhus University;

The Parker Institute, Copenhagen University Hospital. *Email:* george.luta@georgetown.edu

³Division of Biostatistics, Institute of Environmental Medicine, Karolinska Institutet;

Division of Mathematical Statistics, Department of Mathematics, Stockholm University. *Email:* matteo.bottai@ki.se

⁴Department of Economics, University of Waterloo. *Email:* pchause@uwaterloo.ca

⁵Department of Biostatistics, School of Public Health, Boston University. *Email:* doros@bu.edu

⁶Department of Statistics, University of South Carolina. *Email:* pena@stat.sc.edu

Contents

1	Introduction	2
2	MALP: Known Parameters	4
3	Estimated MALP: Unknown Parameters	7
3.1	Consistency and Asymptotic Normality	8
3.2	Illustration for the Simple Case	11
4	Empirical Studies on Estimated MALP	12
4.1	Computer Experiment 1	12
4.2	Computer Experiment 2	14
5	Confidence and Prediction Intervals	17
5.1	Computational Approaches for Standard Errors	17
5.2	Interval Estimation of MALP	18
5.3	Prediction Intervals for $Y(x_0)$	19
6	Illustrative Data Analyses	20
6.1	Eye Data Set	20
6.2	Body fat Data Set	23
7	Concluding Remarks	24
A	Appendix Proofs	28
A.1	Proof of Theorem 1	28
A.2	Proof of Theorem 2	30
A.3	Proof of Theorem 3	38
B	Appendix Additional Computer Experiments	40
B.1	Computer Experiment 1: MALP with $p = 2$	40
B.2	Computer Experiment 1: LSLP with $p = 1$	42
B.3	Computer Experiment 3	42
B.4	Computer Experiment 4	44
C	Appendix Forms of Confidence Intervals	46
D	Appendix Body Fat Data Set Description	47

1 Introduction

The classical correlation coefficient introduced by Galton [12] and mathematically formulated by Pearson [24], hence nowadays called Pearson’s correlation coefficient (PCC), continues to be one of the most-used statistical tools as it provides a quantitative measure of the degree of linear association between two random variables, see Lee Rodgers and Nicewander [19], Stigler [30] for its historical account. With its simple mathematical formulation and low computational cost, its importance still persists in the era of Big Data where researchers have to deal with a large number of variables and/or a large number of observations. While no one doubts the pervasive utility of the PCC, there are certain situations where researchers are more interested in the degree of agreement from the vantage point of the 45° line through the origin, such as in calibration, imputation, and linear equating. In such situations, the PCC may not be the most appropriate measure since it views the degree of linear association from a vantage point that could be any line.

Lin [20] introduced a measure of agreement called the concordance correlation coefficient (CCC). For a bivariate random vector (X, Y) with mean vector (μ_X, μ_Y) and covariance matrix $\begin{bmatrix} \sigma_X^2 & \sigma_{XY} \\ \sigma_{XY} & \sigma_Y^2 \end{bmatrix}$, so has PCC $\rho = \frac{\sigma_{XY}}{\sigma_X \sigma_Y}$, then the CCC between X and Y is defined below.

Definition 1. *Lin's concordance correlation coefficient (CCC) between random variables X and Y that have the same units is*

$$\text{CCC}[X, Y] = \rho^c := 1 - \frac{\text{E}[(X - Y)^2]}{\sigma_X^2 + \sigma_Y^2 + (\mu_X - \mu_Y)^2} = \frac{2\rho\sigma_X\sigma_Y}{\sigma_X^2 + \sigma_Y^2 + (\mu_X - \mu_Y)^2}. \quad (1)$$

In the definition, aside from having the same units, X and Y will usually be measurements of the same characteristic. In this paper, we use ρ and ρ^c instead of ρ_{XY} and ρ_{XY}^c whenever the correlations are between the variables X and Y ; however, the subscripts are specified in other situations. Observe that $\text{E}[(X - Y)^2]$ is twice the expected perpendicular squared Euclidean distance from the 45° line of the random point (X, Y) , hence it is a measure of the degree of concordance between X and Y , with a small absolute value indicative of high concordance. Thus, geometrically speaking, ρ^c measures a particular linear association of X and Y from the vantage point of the 45° line through the origin. The following remark provides some properties of the CCC (see Lin [20]) in relation to the PCC which will be useful later.

Remark 1. *The CCC satisfies the properties: (i) $-1 \leq \rho^c \leq 1$; (ii) $\rho = 0$ if and only if $\rho^c = 0$; and (iii) $|\rho^c| \leq |\rho|$ with equality holding if and only if $\mu_X = \mu_Y$ and $\sigma_X^2 = \sigma_Y^2$.*

Since introduced by Lin [20, 21], the CCC has been used to measure agreement in reproducibility, assay validation, and other types of studies. The results were generalized to both continuous and categorical variables as well as with random and fixed covariates in Lin et al. [22, 23]. For example, in ophthalmology, Abedi et al. [1] developed a conversion formula between the measurements obtained from two optical coherence tomography (OCT): Stratus OCT (conventional approach) and Cirrus OCT (advanced approach); see Figure 1 for the scatter plot of the paired OCT sample data in Abedi et al. [1]. Their formula was developed to maximize the CCC between the two OCT measurements. In the current paper, we extend this idea of using the CCC to develop a predictor (or, a conversion formula, in the case of Abedi et al. [1]'s setting) of Y based on X , which may be multi-dimensional. That is, we consider predictors $\tilde{Y}(X)$ of Y , based on X , in some function class \mathcal{H} , such as the class of linear predictors in X . Then the goal is to find the optimal predictor $\tilde{Y}^* \in \mathcal{H}$ that maximizes the CCC between Y and \tilde{Y} . Since CCC is a measure of agreement, the resulting optimal predictor is called a maximum agreement predictor in the class \mathcal{H} , called the $\text{MAP}_{\mathcal{H}}$. When \mathcal{H} is the class of all possible predictors with finite variance, we simply call $\text{MAP}_{\mathcal{H}}$ as the MAP. In particular, if \mathcal{H} is the class of linear predictors, say \mathcal{H}_{LP} , then the predictor will be called the maximum agreement linear predictor (MALP). For a simple linear case with one-dimensional X , so $\mathcal{H}_{SLP} = \{\tilde{Y} : \tilde{Y}(x) = \alpha + x\beta\}$, the resulting MALP provides a comparable form to the classical

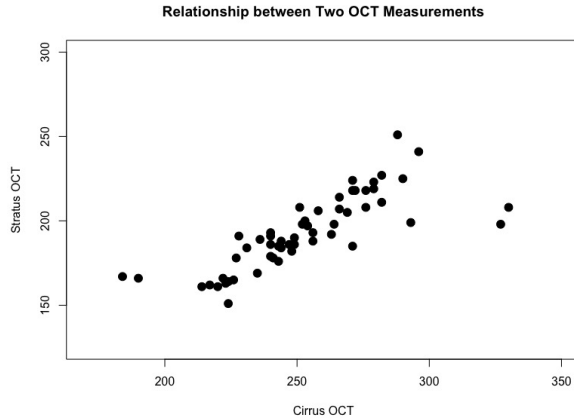


Figure 1: The scatter plot between Stratus and Cirrus OCTs based on 56 observations in the data set in Abedi et al. [1].

least-squares linear predictor \tilde{Y}^\dagger , which is the linear predictor $\tilde{Y}(X) = \alpha + \beta X$ minimizing the mean-squared prediction error (MSPE): $\tilde{Y} \mapsto E[(Y - \tilde{Y}(X))^2]$, where expectation is with respect to the joint distribution of (Y, X) . When the parameters are known, these two predictors, for an X that is one-dimensional, are given by

$$\tilde{Y}^*(x_0) = \mu_y + \text{Sgn}\{\rho\} \left(\frac{\sigma_y}{\sigma_x}\right) (x_0 - \mu_x) \text{ and } \tilde{Y}^\dagger(x_0) = \mu_y + \rho \left(\frac{\sigma_y}{\sigma_x}\right) (x_0 - \mu_x), \quad (2)$$

where $\text{Sgn}(a) = \{-1, 0, +1\}$ according to whether $a \{<, =, >\} 0$, respectively. In Fayers and Hays [11], the form of the MALP in (2) has appeared as a mapping from the space of values of a source instrument to the equivalent space of values of a target instrument in a health science setting. We also mention that the MALP form in (2) has been previously obtained in regression settings under different geometrical motivations: geometric mean regression (see Draper and Yang [9]), least-triangle regression (see Barker et al. [2]), or reduced major-axis regression (see, Kermack and Haldane [17], Smith [29]).

2 MALP: Known Parameters

Let $(\Omega, \mathcal{F}, \mathbf{P})$ be the probability space on which all random entities are defined. We will be concerned with the random vector $(X, Y) : (\Omega, \mathcal{F}) \rightarrow (\mathbb{R}^{p+1}, \mathcal{B}^{p+1})$, where $X = (X_1, \dots, X_p)$ is a p -dimensional random row vector, while Y is one-dimensional, and with \mathcal{B}^{p+1} the Borel sets of \mathbb{R}^{p+1} . Let $F = F_{(X,Y)}$ be the induced joint distribution function of (X, Y) : $F(x, y) = \mathbf{P}\{X \leq x; Y \leq y\}$. Furthermore, we assume that for each $i = 1, \dots, p$, we have $E[X_i^4] < \infty$ and $E[Y^4] < \infty$. In this section, we consider the construction of predictor functions for Y , given $X = x$. For our nomenclature, we will only call a function a *predictor* if its value is computable, given $X = x$, so it

does not depend on *unknown* quantities. We denote the first- and second-order moments of (X, Y) by $\mu_Y = \mathbb{E}[Y]$, $\mu_X = \mathbb{E}[X]$, $\sigma_Y^2 = \text{Var}[Y]$, $\Sigma_{YX} = \text{Cov}[Y, X]$, and $\Sigma_{XX} = \text{Cov}[X, X]$, where Σ_{XX} is assumed to be of full rank. In the sequel, we will write $\text{Cov}[X, X]$ as just $\text{Cov}[X]$. Given $\tilde{Y} \in \mathcal{H}$, where \mathcal{H} is a class of predictors of Y based on X , we define the corresponding moments, if they exist: $\mu_{\tilde{Y}} = \mathbb{E}[\tilde{Y}(X)]$, $\sigma_{\tilde{Y}}^2 = \text{Var}[\tilde{Y}(X)]$, and $\sigma_{Y\tilde{Y}} = \text{Cov}[Y, \tilde{Y}(X)]$. Then, the CCC between Y and \tilde{Y} from (1) is

$$\text{CCC}[Y, \tilde{Y}] = \rho_{Y\tilde{Y}}^c = \frac{2\sigma_{Y\tilde{Y}}}{\sigma_{\tilde{Y}}^2 + \sigma_Y^2 + (\mu_Y - \mu_{\tilde{Y}})^2}. \quad (3)$$

To obtain an optimal predictor in the sense of maximizing agreement, the idea is to find a predictor in the specified class \mathcal{H} that will maximize $\text{CCC}[Y, \tilde{Y}]$. Two classes of predictor functions that are of main interest are the class of linear predictors given by

$$\mathcal{H}_{\text{LP}} = \{\tilde{Y} : \mathbb{R}_p \rightarrow \mathbb{R} \mid \tilde{Y}(x) = \alpha + x\beta : (\alpha, \beta) \in \mathbb{R} \times \mathbb{R}_p\}, \quad (4)$$

where β is a column vector; and the more general class of predictors given by

$$\mathcal{H}_{\text{P}} = \{\tilde{Y} : \mathbb{R}_p \rightarrow \mathbb{R} \mid \mathbb{E}[\tilde{Y}^2(X)] < \infty\}.$$

In the developments below, we first assume that the parameters are known.

Definition 2. *The maximum agreement linear predictor (MALP), denoted by $\tilde{Y}^*(x) = \tilde{Y}^*(x; \alpha, \beta)$, is the best linear predictor (BLP) in \mathcal{H}_{LP} based on the CCC criterion, so that $\rho_{Y\tilde{Y}^*}^c = \sup_{\tilde{Y} \in \mathcal{H}_{\text{LP}}} \rho_{Y\tilde{Y}}^c$. Similarly, the maximum agreement predictor (MAP) arises when the maximization above is performed over the space \mathcal{H}_{P} .*

There is the question of whether there is a unique MALP in \mathcal{H}_{LP} . Note that this is not a trivial issue since when one tries to find a predictor by maximizing the PCC, there are an infinite number of maximizers, hence non-uniqueness ensues. Theorem 1 below provides an affirmative answer to this uniqueness question and presents the explicit form of this MALP.

Theorem 1. *The MALP, $\tilde{Y}^*(x)$, in Definition 2 is unique and has the form $\tilde{Y}^*(x) = \alpha^* + x\beta^*$, where*

$$\beta^* = \frac{\sigma_Y}{\sqrt{\Sigma_{YX}\Sigma_{XX}^{-1}\Sigma_{XY}}} \Sigma_{XX}^{-1}\Sigma_{XY} \quad \text{and} \quad \alpha^* = \mu_Y - \mu_X\beta^*,$$

so that

$$\tilde{Y}^*(x) = \mu_Y + (x - \mu_X) \frac{\sigma_Y}{\sqrt{\Sigma_{YX}\Sigma_{XX}^{-1}\Sigma_{XY}}} \Sigma_{XX}^{-1}\Sigma_{XY} = \mu_Y + (x - \mu_X) \frac{1}{\gamma} \Sigma_{XX}^{-1}\Sigma_{XY}. \quad (5)$$

In addition, the achieved maximum CCC has the value $\rho_{Y\tilde{Y}^*}^c = \gamma \equiv \frac{\sqrt{\Sigma_{YX}\Sigma_{XX}^{-1}\Sigma_{XY}}}{\sigma_Y}$.

Proof. See Section 1.1 in the Appendix. □

We point out that Theorems 1 and 2 in Bottai et al. [4] proved the uniqueness of the MAP in \mathcal{H}_p and that both the MAP and the least-squares predictor also maximize the PCC among the predictors in \mathcal{H}_p .

Remark 2. *The following remarks regarding the MALP relate it to the least-squares predictor and also presents some results from Bottai et al. [4] and Christensen [6].*

i) Let $\tilde{Y}^\dagger(x)$ be the least-squares linear predictor (LSLP) of Y , given $X = x$, in the class \mathcal{H}_{LP} , the usual multiple linear regression model. This is given by

$$\tilde{Y}^\dagger(x) = \mu_Y + (x - \mu_X)\Sigma_{XX}^{-1}\Sigma_{XY}, \quad (6)$$

and is usually referred to as the least-squares multiple linear regression predictor.

ii) From (5) and (6), observe that $\sigma_{\tilde{Y}^\dagger}^2 = \text{Var}[\tilde{Y}^\dagger(X)] = \Sigma_{YX}\Sigma_{XX}^{-1}\Sigma_{XY}$ and $\sigma_{\tilde{Y}^*}^2 = \text{Var}[\tilde{Y}^*(X)] = \sigma_Y^2$. Thus, with $\rho_{\tilde{Y}^\dagger} = \sigma_{\tilde{Y}^\dagger}/\sigma_Y = \gamma$, note that the MALP can be expressed in terms of the LSLP via $\tilde{Y}^*(x) = \left(1 - \frac{1}{\gamma}\right)\mu_Y + \frac{1}{\gamma}\tilde{Y}^\dagger(x)$; see also Bottai et al. [4, equation (11)]. This amounts to a re-centering and a re-scaling of the LSLP so its mean is equal to $E(Y)$ and its variance is equal to $\text{Var}(Y)$. This is referred to as the ‘‘calibration approach’’ to obtaining the MALP from the LSLP, and this provides a computational advantage in practice since $\tilde{Y}^\dagger(x)$ can be obtained conveniently from existing statistical packages.

iii) Whereas $\tilde{Y}^*(x)$ is expressible as an affine transformation of μ_Y and $\tilde{Y}^\dagger(x)$ weighted by the terms with $\frac{1}{\gamma}$, $\tilde{Y}^\dagger(x)$ is expressible as a convex combination of μ_Y and $\tilde{Y}^*(x)$, and as a shrinkage (since $0 \leq \gamma < 1$) towards μ_Y such that $\tilde{Y}^\dagger(x) = (1 - \gamma)\mu_Y + \gamma\tilde{Y}^*(x) = \mu_Y + \gamma[\tilde{Y}^*(x) - \mu_Y]$.

iv) The maximum CCC in Theorem 1 is equal to the Pearson correlation coefficient between Y and \tilde{Y}^* , or between Y and \tilde{Y}^\dagger (see also Bottai et al. [4, Theorem 3]). That is, $\rho_{\tilde{Y}^*}^c = \rho_{Y\tilde{Y}^*} = \rho_{Y\tilde{Y}^\dagger} = \sigma_{\tilde{Y}^\dagger}/\sigma_Y = \gamma$.

v) Though not the focus of this paper, we state at this point the expression of the more general MAP obtained in Bottai et al. [4]. This is the predictor

$$\delta^{**}(x) = \left(1 - \frac{1}{\gamma^{**}}\right)E(Y) + \frac{1}{\gamma^{**}}E(Y|X = x)$$

with $\gamma^{**} = +\sqrt{\frac{\text{Var}[E(Y|X)]}{\text{Var}(Y)}}$. Note that the forms of MAP and the MALP coincide when $F_{(X,Y)}$ is multivariate normal, see Bottai et al. [4, Example 1]. In fact, more generally, when $E(Y|X = x) = \alpha + x\beta$, that is, the conditional mean of Y , given $X = x$, is linear in x , then the MALP and MAP coincide. This MAP, aside from maximizing the $\text{CCC}(Y, \delta)$ among all $\delta \in \mathcal{H}_p$, can also be obtained by minimizing the mean-squared prediction error between the

predictor and the predictand under the equal mean and variance constraints among all predictors in \mathcal{H}_p ; see Christensen [6]. This particular constrained optimization idea is also found in the constrained kriging approach in spatial statistics; see Cressie [7]. In Ghosh [13], the form of the MAP has also appeared in a simultaneous Bayesian estimation context, where it is called a constrained Bayes predictor.

3 Estimated MALP: Unknown Parameters

In the preceding developments, we assumed that the parameters are known. However, this will be a very rare situation in practice, hence there is a need to replace the unknown parameters in the MALP and the LSLP by their estimators based on sample data to obtain (implementable) predictors. Thus, suppose that $[\mathbf{X}, \mathbf{Y}]$ is the $n \times (p + 1)$ matrix formed from a random sample $\{(X_i, Y_i)\}_{i=1}^n$ of size n . The goal is to predict the value of an unobserved Y_0 associated with a realization $X_0 = x_0$. With $\mathbf{1}_n$ denoting an $n \times 1$ column vector of 1's, I the n -dimensional identity matrix, $J = \mathbf{1}_n \mathbf{1}_n^\top$ the n -dimensional matrix of 1's, and \otimes denoting Kronecker product, the sample moments could be expressed via:

$$\begin{aligned} \bar{X} &= \frac{1}{n} \mathbf{1}_n^\top \mathbf{X}; & \bar{Y} &= \frac{1}{n} \mathbf{1}_n^\top \mathbf{Y}; & \mathbf{S}_{\mathbf{X}\mathbf{X}} &= \frac{1}{n-1} (\mathbf{X} - \mathbf{1}_n \otimes \bar{X})^\top (\mathbf{X} - \mathbf{1}_n \otimes \bar{X}); \\ S_Y^2 &= S_{\mathbf{Y}\mathbf{Y}} = \frac{1}{n-1} (\mathbf{Y} - \mathbf{1}_n \bar{Y})^\top (\mathbf{Y} - \mathbf{1}_n \bar{Y}); & \mathbf{S}_{\mathbf{X}\mathbf{Y}} &= \mathbf{S}_{\mathbf{Y}\mathbf{X}}^\top = \frac{1}{n-1} (\mathbf{X} - \mathbf{1}_n \otimes \bar{X})^\top (\mathbf{Y} - \mathbf{1}_n \bar{Y}). \end{aligned} \quad (7)$$

We could now obtain an estimator of the MALP in (5) via

$$\hat{Y}^*(x_0; [\mathbf{X}, \mathbf{Y}]) = \bar{Y} + (x_0 - \bar{X}) \frac{1}{\hat{\gamma}} \mathbf{S}_{\mathbf{X}\mathbf{X}}^{-1} \mathbf{S}_{\mathbf{X}\mathbf{Y}}. \quad (8)$$

Notice that $\hat{\gamma} = \sqrt{\mathbf{S}_{\mathbf{Y}\mathbf{X}} \mathbf{S}_{\mathbf{X}\mathbf{X}}^{-1} \mathbf{S}_{\mathbf{X}\mathbf{Y}}} / S_Y$ is the sample's multiple correlation coefficient between Y and X (its square is the sample multiple coefficient of determination) and $\mathbf{S}_{\mathbf{X}\mathbf{X}}^{-1} \mathbf{S}_{\mathbf{X}\mathbf{Y}}$ is the multiple regression coefficient without the intercept term. As a special case with $p = 1$ (i.e., the simple case), the form can be simplified as follows:

$$\hat{Y}^*(x_0; [\mathbf{X}, \mathbf{Y}]) = \bar{Y} + (x_0 - \bar{X}) \text{Sgn}\{R_{\mathbf{X}\mathbf{Y}}\} (S_Y / S_X), \quad (9)$$

where $R_{\mathbf{X}\mathbf{Y}} = S_{\mathbf{X}\mathbf{Y}} / (S_X S_Y)$ with $S_X = \sqrt{S_{\mathbf{X}\mathbf{X}}}$. We can similarly construct an estimator of the LSLP in (6) given by

$$\hat{Y}^\dagger(x_0; [\mathbf{X}, \mathbf{Y}]) = \bar{Y} + (x_0 - \bar{X}) \mathbf{S}_{\mathbf{X}\mathbf{X}}^{-1} \mathbf{S}_{\mathbf{X}\mathbf{Y}}, \quad (10)$$

which, when $p = 1$, becomes

$$\hat{Y}^\dagger(x_0; [\mathbf{X}, \mathbf{Y}]) = \bar{Y} + (x_0 - \bar{X}) R_{\mathbf{X}\mathbf{Y}} (S_Y / S_X). \quad (11)$$

3.1 Consistency and Asymptotic Normality

We investigate the properties of the estimators $\hat{Y}^*(x_0; [\mathbf{X}, \mathbf{Y}])$ and $\hat{Y}^\dagger(x_0; [\mathbf{X}, \mathbf{Y}])$ of the MALP and LSLP, respectively, at a fixed point x_0 . Except for the finiteness of fourth moments stated earlier, at this point we are not imposing a specific joint distribution F , such a multivariate normality, on (Y, X) . Note that these are estimators of $\tilde{Y}^*(x_0)$ and $\tilde{Y}^\dagger(x_0)$, respectively. Since $(\bar{X}, \bar{Y}, \mathbf{S}_{XX}, \mathbf{S}_{XY}, S_{YY})$, the method-of-moments estimator, is a consistent estimator of $(\mu_X, \mu_Y, \Sigma_{XX}, \Sigma_{XY}, \Sigma_{YY})$ as $n \rightarrow \infty$, it follows that $\hat{Y}^*(x_0; [\mathbf{X}, \mathbf{Y}])$ is consistent for $\tilde{Y}^*(x_0)$ and $\hat{Y}^\dagger(x_0; [\mathbf{X}, \mathbf{Y}])$ is consistent for $\tilde{Y}^\dagger(x_0)$ as $n \rightarrow \infty$. For the asymptotic normality, we utilize the U -statistics approach [14] with p -dimensional row vector X . While this approach provides the general result with no distributional assumptions on F , it may be difficult to obtain a closed form of the asymptotic variance for general p . To supplement the result obtained using U -statistics and in order to obtain closed-form expressions, we also present a result that provides the form of the asymptotic variance in the special case when F is a $(p + 1)$ -dimensional multivariate normal distribution.

Note first that the components of the vector of estimators $(\bar{X}, \bar{Y}, \mathbf{S}_{XX}, \mathbf{S}_{XY}, S_{YY})$ are U -statistics [14], with those for \bar{X} and \bar{Y} having unbiased kernels of order one; while those for \mathbf{S}_{XX} , \mathbf{S}_{XY} , and S_{YY} having unbiased kernels of order two. The symmetric kernels in terms of two observations (x_1, y_1) and (x_2, y_2) with $\{(x_i, y_i) = (x_{ij}, y_{ij})_{j=1}^p, i = 1, 2\}$ can be combined into a vector form:

$$\mathbf{h} = \left[(h_{1j})_{j=1}^p, h_2, (h_{3jl})_{1 \leq j \leq l \leq p}, (h_{4j})_{j=1}^p, h_5 \right], \quad (12)$$

where the individual terms, given j or $j \leq l$, are

$$\begin{aligned} h_{1j}((x_1, y_1), (x_2, y_2)) &= \frac{(x_{1j} + x_{2j})}{2}; & h_2((x_1, y_1), (x_2, y_2)) &= \frac{(y_1 + y_2)}{2}; \\ h_{3jl}((x_1, y_1), (x_2, y_2)) &= \frac{(x_{1j} - x_{2j})(x_{1l} - x_{2l})}{2}; & h_{4j}((x_1, y_1), (x_2, y_2)) &= \frac{(x_{1j} - x_{2j})(y_1 - y_2)}{2}; \\ h_5((x_1, y_1), (x_2, y_2)) &= \frac{(y_1 - y_2)^2}{2}. \end{aligned}$$

Note that \mathbf{h} is a kernel for the parameter vector $\theta = \left[(\mu_{X_j})_{j=1}^p, \mu_Y, (\sigma_{X_j X_l})_{1 \leq j \leq l \leq p}, (\sigma_{X_j Y})_{j=1}^p, \sigma_Y^2 \right]$. For notation, let $\text{VEC}(\cdot)$ be the operator that converts a vector/matrix into a column vector, with the caveat that for a symmetric matrix, we only use the upper-triangular component of the matrix, e.g., $\text{VEC} \left(\begin{bmatrix} a & b \\ b & c \end{bmatrix} \right) = (a, b, c)^\top$. Note that for symmetric matrices, VEC is the so-called VECH operator. Thus, if we let

$$\mathbf{T} \equiv \text{VEC}(\bar{X}, \bar{Y}, \mathbf{S}_{XX}, \mathbf{S}_{XY}, S_{YY}) \quad \text{and} \quad \theta \equiv \text{VEC}(\mu_X, \mu_Y, \Sigma_{XX}, \Sigma_{XY}, \Sigma_{YY}),$$

we have that $E[\mathbf{h}((X_1, Y_1), (X_2, Y_2))] = \theta$ and \mathbf{T} could be expressed as a U -statistic via

$$\mathbf{T} \equiv T((X_1, Y_1), \dots, (X_n, Y_n)) = \frac{1}{\binom{n}{2}} \sum_{1 \leq i < k \leq n} \mathbf{h}((X_i, Y_i), (X_k, Y_k)).$$

Observe that \mathbf{h} , \mathbf{T} , and θ are $\left(\frac{(p+4)(p+1)}{2}\right)$ -dimensional vectors.

The One-Sample Multivariate U -Statistics Theorem (see Serfling [27]) could then be invoked to conclude, as $n \rightarrow \infty$ and under the finite fourth moment condition on the components of X and Y , that \mathbf{T} is asymptotically multivariate normal with mean vector θ and asymptotic covariance matrix $\frac{4}{n}\Sigma_h$, for some Σ_h induced by \mathbf{h} , that is,

$$\sqrt{n}(\mathbf{T} - \theta) \xrightarrow{d} \mathcal{N}(\mathbf{0}, 4\Sigma_h). \quad (13)$$

Letting $\tilde{\mathbf{h}}((x_1, y_1)) = E[\mathbf{h}((x_1, y_1), (X_2, Y_2))]$, then $\Sigma_h = \text{Cov}[\tilde{\mathbf{h}}((X_1, Y_1)), \tilde{\mathbf{h}}((X_1, Y_1))]$. Similar to \mathbf{h} in (12), the vector $\tilde{\mathbf{h}}$ consists of the individual terms, given j or $j \leq l$, are:

$$\begin{aligned} \tilde{h}_{1j}((x_1, y_1)) &= \frac{(x_{1j} + \mu_{x_j})}{2}; & \tilde{h}_2((x_1, y_1)) &= \frac{(y_1 + \mu_Y)}{2}; \\ \tilde{h}_{3jl}((x_1, y_1)) &= \frac{[(x_{1j} - \mu_{x_j})(x_{1l} - \mu_{x_l}) + \sigma_{x_j x_l}]}{2}; & \tilde{h}_{4j}((x_1, y_1)) &= \frac{[(x_{1j} - \mu_{x_j})(y_1 - \mu_Y) + \sigma_{x_j Y}]}{2}; \\ \tilde{h}_5((x_1, y_1)) &= \frac{[(y_1 - \mu_Y)^2 + \sigma_Y^2]}{2}. \end{aligned}$$

Under specific distributional assumptions, such as the multivariate normal distribution for (X, Y) , closed-form formulas for Σ_h may be obtained, possibly tediously. Since $\hat{Y}^\dagger(x_0; [\mathbf{X}, \mathbf{Y}])$ and $\hat{Y}^\star(x_0; [\mathbf{X}, \mathbf{Y}])$ are functions of \mathbf{T} , albeit in a complicated manner, we could then invoke the Multivariate Delta-Method to conclude that both are asymptotically normal with respective means of $\tilde{Y}^\star(x_0)$ and $\tilde{Y}^\dagger(x_0)$ and asymptotic variances of forms

$$\frac{1}{n}\sigma_{\text{MA}}^2 = \frac{4}{n}(\nabla g_{\text{M}}(\theta))^\top \Sigma_h (\nabla g_{\text{M}}(\theta)) \quad \text{and} \quad \frac{1}{n}\sigma_{\text{LS}}^2 = \frac{4}{n}(\nabla g_{\text{L}}(\theta))^\top \Sigma_h (\nabla g_{\text{L}}(\theta)),$$

where g_{M} and g_{L} are the mappings such that $\hat{Y}^\star(x_0; [\mathbf{X}, \mathbf{Y}]) = g_{\text{M}}(\mathbf{T})$ and $\hat{Y}^\dagger(x_0; [\mathbf{X}, \mathbf{Y}]) = g_{\text{L}}(\mathbf{T})$, and ∇ is the gradient operator with respect to the arguments of the mapping. Thus, for instance, $\nabla g_{\text{M}}(\theta) = \frac{\partial}{\partial \mathbf{t}} g_{\text{M}}(\mathbf{t})|_{\mathbf{t}=\theta}$. As a result, the following asymptotic normality results hold:

$$\sqrt{n} \left(\hat{Y}^\star(x_0; [\mathbf{X}, \mathbf{Y}]) - \tilde{Y}^\star(x_0) \right) \xrightarrow{d} \mathcal{N}(\mathbf{0}, \sigma_{\text{MA}}^2) \quad \text{and} \quad \sqrt{n} \left(\hat{Y}^\dagger(x_0; [\mathbf{X}, \mathbf{Y}]) - \tilde{Y}^\dagger(x_0) \right) \xrightarrow{d} \mathcal{N}(\mathbf{0}, \sigma_{\text{LS}}^2). \quad (14)$$

We mention that the U -statistics approach has been used to establish the asymptotic normality of the sample PCC, see Serfling [27, Chapter 3.4] and also for the sample CCC as in King and Chinchilli [18, Appendix II]. As mentioned earlier, with the U -statistics approach, the form of the asymptotic variance for the general p case may be hard to obtain. However, when F is a

$(p + 1)$ -dimensional multivariate normal distribution, the following theorem provides the closed-form expressions of the asymptotic variances of the estimated MALP and LSLP which, surprisingly, are of simple forms for any value of p .

Theorem 2. *If $\{(X_i, Y_i), i = 1, \dots, n\}$ is a random sample from any multivariate distribution F with finite fourth moments and with mean vector $\mu = (\mu_X, \mu_Y)$ and a nonsingular covariance matrix $\Sigma = \begin{bmatrix} \Sigma_{XX} & \Sigma_{XY} \\ \Sigma_{YX} & \sigma_Y^2 \end{bmatrix}$ with $\Sigma_{YX} \neq 0$, then the estimated MALP in (8) and the estimated LSLP in (10) satisfy, as $n \rightarrow \infty$,*

$$\hat{Y}^*(x_0) \sim \mathcal{AN} \left(\tilde{Y}^*(x_0), \frac{1}{n} \sigma_{MA}^2(x_0) \right) \quad \text{and} \quad \hat{Y}^\dagger(x_0) \sim \mathcal{AN} \left(\tilde{Y}^\dagger(x_0), \frac{1}{n} \sigma_{LS}^2(x_0) \right).$$

If F is restricted to be a multivariate normal distribution, then the asymptotic variances can be expressed as follows:

$$\sigma_{MA}^2(x_0) = \sigma_Y^2(1 - \gamma^2) \left[\frac{2}{1 + \gamma} + \frac{1}{\gamma^2} (x_0 - \mu_X) \Sigma_{XX}^{-1} (x_0 - \mu_X)^\top - \frac{(1 - \gamma^2)}{\sigma_Y^2 \gamma^4} [\Sigma_{YX} \Sigma_{XX}^{-1} (x_0 - \mu_X)^\top]^2 \right]; \quad (15)$$

$$\sigma_{LS}^2(x_0) = \sigma_Y^2(1 - \gamma^2) [1 + (x_0 - \mu_X) \Sigma_{XX}^{-1} (x_0 - \mu_X)^\top], \quad (16)$$

where $\gamma = \sqrt{\Sigma_{YX} \Sigma_{XX}^{-1} \Sigma_{XY}} / \sigma_Y$. Furthermore, when $p = 1$, so that $\gamma = |\rho|$, then

$$\sigma_{MA}^2(x_0) = \sigma_Y^2(1 - \rho^2) \left[\frac{2}{1 + |\rho|} + \left(\frac{x_0 - \mu_X}{\sigma_X} \right)^2 \right].$$

Proof. See Section 1.2 in the Appendix. □

Remark 3. *A few comments regarding the asymptotic normality results in Theorem 2 when F is multivariate normal:*

i) *By Cauchy-Schwartz Inequality, we find that $[\Sigma_{YX} \Sigma_{XX}^{-1} (x_0 - \mu_X)^\top]^2 \leq \{(x_0 - \mu_X) \Sigma_{XX}^{-1} (x_0 - \mu_X)^\top\} (\sigma_Y^2 \gamma^2)$. As a consequence, we have the inequality, for $p \geq 1$,*

$$\begin{aligned} \sigma_{MA}^2(x_0) &\geq \sigma_Y^2(1 - \gamma^2) \left[\frac{2}{1 + \gamma} + (x_0 - \mu_X) \Sigma_{XX}^{-1} (x_0 - \mu_X)^\top \right] \\ &\stackrel{\gamma \leq 1}{\geq} \sigma_Y^2(1 - \gamma^2) [1 + (x_0 - \mu_X) \Sigma_{XX}^{-1} (x_0 - \mu_X)^\top] = \sigma_{LS}^2(x_0). \end{aligned}$$

Thus, we have shown that, for $p \geq 1$, we have $\sigma_{MA}^2(x_0) \geq \sigma_{LS}^2(x_0)$.

ii) *Note that the term $\sigma_Y^2(1 - \gamma^2)$ is the conditional variance of Y , given $X = x_0$, which does not depend on x_0 by the homoscedasticity property of the multivariate normal distribution; whereas, the term $(x_0 - \mu_X) \Sigma_{XX}^{-1} (x_0 - \mu_X)^\top$ is the squared Mahalanobis distance between x_0 and μ_X .*

iii) *The accuracy of the normal approximation for a given sample size depends on the value of γ ,*

which is $|\rho|$ when $p = 1$. That is, the smaller the γ the worse the approximation for a given sample size n .

3.2 Illustration for the Simple Case

To demonstrate that we obtain the same expressions under the U -statistics approach and the result in Theorem 2 under multivariate normality, we consider the simple case when $p = 1$. Thus, we assume that

$$\begin{bmatrix} X_i \\ Y_i \end{bmatrix} \stackrel{iid}{\sim} \mathcal{BVN} \left(\begin{bmatrix} \mu_X \\ \mu_Y \end{bmatrix}, \begin{bmatrix} \sigma_X^2 & \sigma_{XY} \\ \sigma_{XY} & \sigma_Y^2 \end{bmatrix} \right), \quad i = 1, \dots, n.$$

While the sample moments related to Y remains the same as in the general case in (7), the sample moments related to X become $\bar{X} = \frac{1}{n} \sum_{i=1}^n X_i$, $S_X^2 = \frac{1}{n-1} \sum_{i=1}^n (X_i - \bar{X})^2$, and $S_{XY} = \frac{1}{n-1} \sum_{i=1}^n (X_i - \bar{X})(Y_i - \bar{Y})$. Then, the estimated MALP for $p = 1$ has the form in (9). In this case, \mathbf{T} , θ , and the covariance matrix $4\Sigma_h = 4\text{Cov}[\tilde{\mathbf{h}}((X_1, Y_1)), \tilde{\mathbf{h}}((X_1, Y_1))]$, obtained using Isserlis' Theorem (see, Isserlis [15]), are given by

$$\mathbf{T} = \begin{bmatrix} \bar{X} \\ \bar{Y} \\ S_X^2 \\ S_{XY} \\ S_Y^2 \end{bmatrix}, \quad \theta = \begin{bmatrix} \mu_X \\ \mu_Y \\ \sigma_X^2 \\ \sigma_{XY} \\ \sigma_Y^2 \end{bmatrix}, \quad \text{and} \quad 4\Sigma_h = \begin{bmatrix} \sigma_X^2 & & & & \\ \sigma_{XY} & \sigma_Y^2 & & & \\ 0 & 0 & 2\sigma_X^4 & & \\ 0 & 0 & 2\sigma_X^2\sigma_{XY} & \sigma_X^2\sigma_Y^2 + \sigma_{XY}^2 & \\ 0 & 0 & 2\sigma_{XY}^2 & 2\sigma_Y^2\sigma_{XY} & 2\sigma_Y^4 \end{bmatrix}. \quad (17)$$

From (9) and (11), we have the mappings

$$g_M(t; x_0) = t_2 + \text{Sgn}(t_4) \sqrt{t_5/t_3} (x_0 - t_1) \quad \text{and} \quad g_L(t; x_0) = t_2 + (t_4/t_3)(x_0 - t_1)$$

for $t = (t_1, t_2, t_3, t_4, t_5)$, with the corresponding gradient vectors

$$d_M(\theta) = \frac{\partial}{\partial t} g_M(t)|_{t=\theta} = \left[-\text{Sgn}(\sigma_{XY}) \frac{\sigma_Y}{\sigma_X}, 1, -(x_0 - \mu_X) \frac{\text{Sgn}(\sigma_{XY})\sigma_Y}{2\sigma_X^3}, 0, (x_0 - \mu_X) \frac{\text{Sgn}(\sigma_{XY})}{2\sigma_X\sigma_Y} \right]^\top;$$

$$d_L(\theta) = \frac{\partial}{\partial t} g_L(t)|_{t=\theta} = \left[-\frac{\sigma_{XY}}{\sigma_X^2}, 1, -(x_0 - \mu_X) \frac{\sigma_{XY}}{\sigma_X^4}, (x_0 - \mu_X) \frac{1}{\sigma_X^2}, 0 \right]^\top.$$

Therefore, by the Multivariate Delta Method and via some simplifications, we obtain the asymptotic means and variances for MALP and LSLP to be

$$\begin{aligned} \mu_{\text{MA}} &= g_M(\theta) = \tilde{Y}^\star(x_0); & \mu_{\text{LS}} &= g_L(\theta) = \tilde{Y}^\dagger(x_0); \\ \frac{1}{n} \sigma_{\text{MA}}^2 &= \frac{4}{n} (d_M(\theta))^\top \Sigma_h (d_M(\theta)) = \frac{1}{n} \sigma_Y^2 (1 - \rho^2) \left\{ \frac{2}{1+|\rho|} + \left(\frac{x_0 - \mu_X}{\sigma_X} \right)^2 \right\}; \\ \frac{1}{n} \sigma_{\text{LS}}^2 &= \frac{4}{n} (d_L(\theta))^\top \Sigma_h (d_L(\theta)) = \frac{1}{n} \sigma_Y^2 (1 - \rho^2) \left\{ 1 + \left(\frac{x_0 - \mu_X}{\sigma_X} \right)^2 \right\}. \end{aligned}$$

Note that since $|\rho|$ is equal to γ when $p = 1$, then these expressions coincide with those in Theorem

2. When $x_0 = 0$, the obtained asymptotic variance for the MALP recovers a related result in Kermack and Haldane [17].

4 Empirical Studies on Estimated MALP

In this section, we present the results of computer experiments to i) assess the quality of the mean and variance approximations provided by the asymptotic mean and variance of the estimated MALP; ii) assess the adequacy of the approximate normality; and iii) assess the quality of MALP and LSLP in terms of CCC, PCC, and MSE (though MSE is actually the ‘mean squared prediction error’ (MSPE)). For these computer experiments, we focus on the simple setting with $p = 1$ where F , the distribution of (X, Y) , is a bivariate normal distribution. However, Section 2 in the Appendix includes the results of the first experiment with $p = 2$ for a trivariate normal distribution, as well as the corresponding results for the estimated LSLP. In addition, it also contains two additional experiments concerning the performance and quality of the normal approximations of the MALP and LSLP, respectively.

4.1 Computer Experiment 1

In the first set of computer experiments, we assign the arbitrarily chosen parameter values ($\mu_X = 5$, $\mu_Y = 5$, $\sigma_X = 2$, $\sigma_Y = 4$, ρ), where ρ is replaced by a value from the set $\{0.05, 0.5, 0.9\}$. Then, given a sample size $n \in \{30, 50, 200\}$, we obtain the vector $x_0 = [x_{0j}]_{j=1}^9$ whose elements are the deciles of the marginal distribution $\mathcal{N}(\mu_X, \sigma_X^2)$ of X . For each replication $l = 1, \dots, \text{MReps}$, a random sample of size n , given by $(X_l, Y_l) = \{(X_{li}, Y_{li})\}_{i=1}^n$, is generated from F , the bivariate normal distribution with the assigned parameters. For this sample, $\hat{Y}_l^*(\cdot; (X_l, Y_l))$ is obtained, and then the predictions $\hat{Y}_{0j}^* = \hat{Y}_l^*(x_{0j}; (X_l, Y_l))$ are computed. For each $j = 1, \dots, 9$, the means, variances, boxplots, and histograms of $\hat{Y}_{0j}^* = \{\hat{Y}_{0jl}^*\}_{l=1}^{\text{MReps}}$ are obtained.

We compare these empirical means and variances with the approximations provided by the asymptotic results in Theorem 2 for different values of n and ρ . Observe that by the Weak Law of Large Numbers (WLLN), as MReps increases, the empirical means and variances will converge in probability to the true means and variances of the \hat{Y}_{0j}^* s. Thus, for this experiment, we want to ascertain how good the asymptotic approximations for the means and variances are for a given combination (n, ρ) . Figure 2 depicts the results pictorially, with the first row being for the means, the second row for the variances, and the third row providing the boxplots but only for the case $n = 200$; while the three columns (panels A, B, C) are for the different values of ρ . For each of these plots, the abscissa shows the values of the x_{0j} ’s. In the first and second rows, the dotted points are the empirical results, whereas the solid curves are the asymptotic approximations. When $\rho = 0.5$ and $\rho = 0.9$ in panel B and panel C, respectively, the asymptotic approximations are adequate, even for $n = 30$, but with a slight degradation for the variance approximation when $n = 30$. Note that

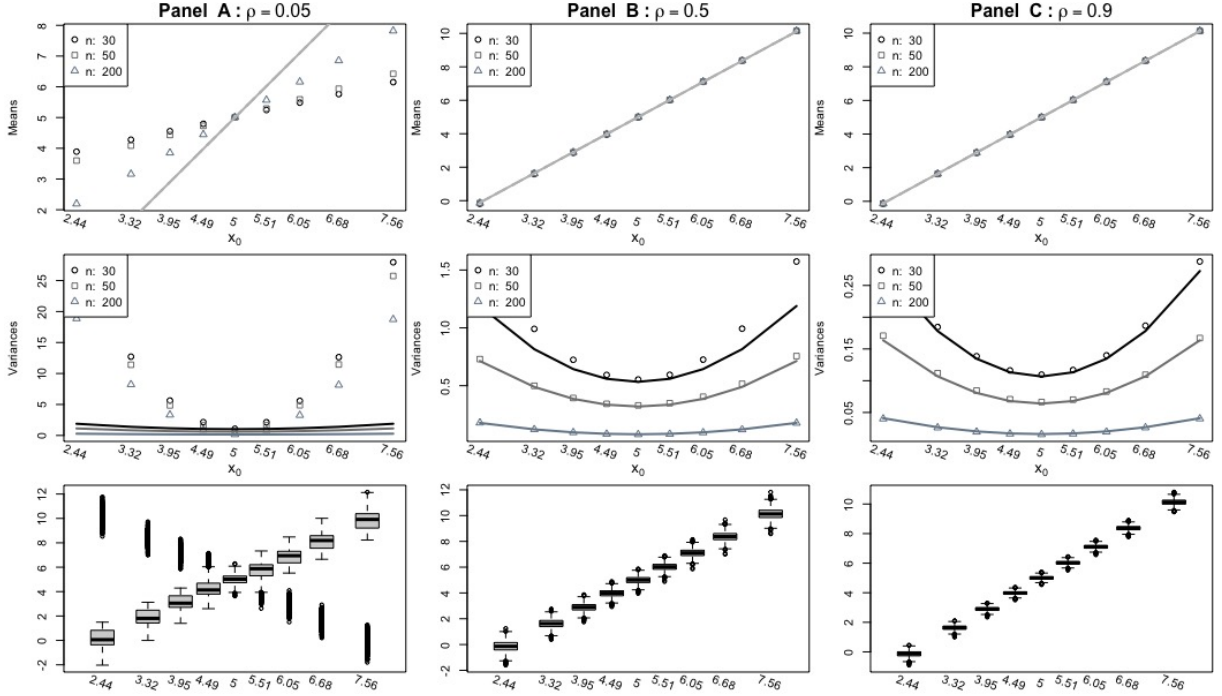


Figure 2: The approximation quality for the estimated MALP for different (ρ, n) at x_0 's: the empirical means and variances (dotted) of \hat{Y}_0^* s with their asymptotic approximations (solid curves). Also depicted are the boxplots for the case where $n = 200$.

in these cases, the boxplots do not anymore show mixture distributions at $n = 200$. When $\rho = 0.05$ in panel A, there is a non-negligible discrepancy between the empirical means and variances with the asymptotic means and variances, even when n is large. The boxplots in the third row also show that the distributions are far from normal. The reason for this is that when ρ is small, the sample correlation coefficient r has a high probability of having the opposite sign as that of ρ , and since for the MALP there is a term involving $\text{Sgn}(r)$, this creates a bifurcation making the sampling distribution of the \hat{Y}_{0j}^* to be a mixture distribution. Of course, when we keep increasing n , the mixture component distribution induced by the oppositely-signed r becomes less likely, since r converges to ρ in probability as $n \rightarrow \infty$.

To examine further the distributional aspects, Figure 3 provides the histograms of the \hat{Y}_{0j}^* at $x_0 = 6.05$, the 70th percentile of the X distribution, for the different values of (n, ρ) . We chose the 70th percentile, instead of the mean or median, in order to illustrate that the sampling distribution of \hat{Y}_{0j}^* could be a mixture of two quite different distributions when ρ is small. So, in each panel, the distribution of \hat{Y}_{0j}^* for $\rho = 0.05$ is bimodal, whereas two other distributions with $\rho = 0.5$ and 0.9 are bell-shaped. But, as n increases, the left component of the mixture becomes less likely and the normal distribution approximation improves. It should be pointed out that a value of $\rho = .05$ is too low when trying to predict Y from X in practical situations. However, to give

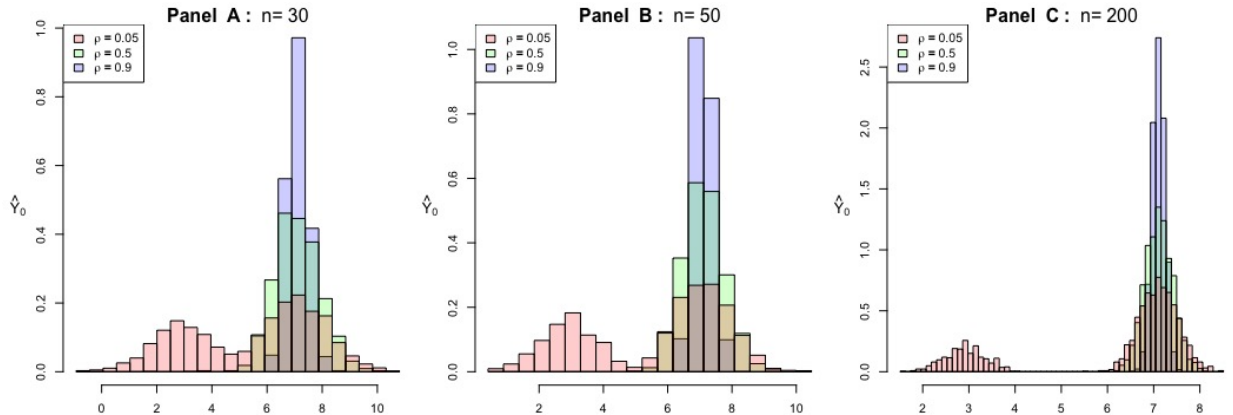


Figure 3: Empirical histograms of the estimated MALP \hat{Y}_0^* s at $x_0 = 6.05$ for different values of (ρ, n) based on 2000 replications.

further insights regarding when the asymptotic expressions for the mean and variance become adequate for small $|\rho|$ -values, we performed additional simulations at $\rho = .05$ and with sample sizes of $n \in \{1000, 3000, 5000\}$. The results of these additional simulation runs in Figure 4 showed that for large sample sizes n and when $|\rho|$ is close to zero, the asymptotic expressions become adequate. When ρ is close to zero and the sample size is not large, the asymptotic expressions should not be used, but instead computational approaches such as the bootstrap or jackknife should be employed instead to estimate standard errors. This is supported by the results of additional simulations we have performed.

We also performed simulations when $p = 2$ and the F distribution is trivariate normal with $\gamma = 0.05, 0.5,$ and 0.9 . While the resulting behaviors are similar to the case with $p = 1$, the bimodalities in the empirical sampling distribution histograms in Panel A (small γ) of Figure 10 in Section 2.1 of the Appendix are less pronounced compared to the case with $p = 1$. A possible explanation for this behavior is that the MALP does not contain the sign function when $p \geq 2$, compared to when $p = 1$, so there is some smoothness with respect to γ . Observe, however, that the histograms for $n = 200$ become closer to being bell-shaped when $|\gamma|$ increases, as can be seen in Panels B and C in Figure 10. For this experiment, the same procedures were done for the estimated LSLP $\hat{Y}_l^\dagger(\cdot; (X_l, Y_l))$ and the results regarding the predictions $\hat{Y}_{0jl}^\dagger = \hat{Y}^\dagger(x_{0j}; (X_l, Y_l))$ are presented in Figures 11 and 12 in Section 2.2 of the Appendix. Observe that since there is no $\text{Sgn}(r)$ term in the LSLP, the asymptotic mean and variance approximations, including the normal approximations, are better compared to the case of the estimated MALP.

4.2 Computer Experiment 2

In this set of experiments, we investigated further the difference between MALP and LSLP, with the performance evaluations done on a test sample data that is independent of the training data,

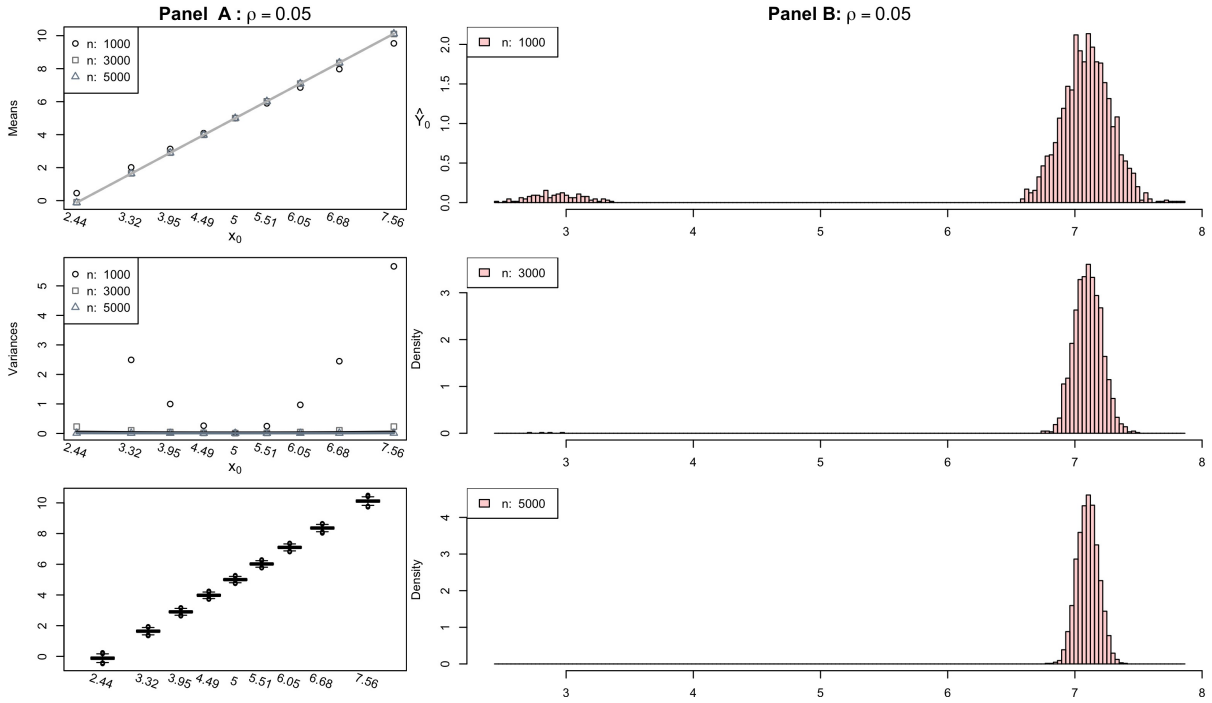
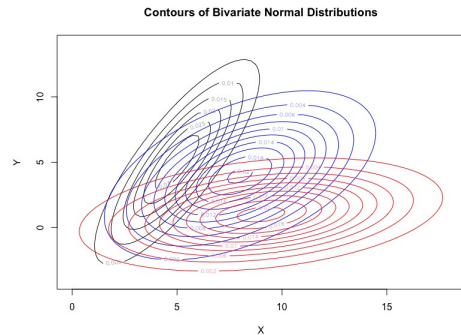


Figure 4: The approximation quality for the MALP for $\rho = 0.05$ and large $n = 1000, 3000, 5000$: Panel A shows the empirical means and variances (dotted) of \hat{Y}_0^\dagger 's with their asymptotic approximations (solid curves), along with the boxplots for the case when $n = 5000$. Panel B presents the empirical histograms of the estimated MALP at $x_0 = 6.05$ for large n 's.

as is usually done in machine learning settings. For the l th replication with $l = 1, \dots, M$ Reps, a random sample $(X_l, Y_l) = \{(X_{li}, Y_{li})\}_{i=1}^n$ of size $n = 100$, and another random sample $(X_{0l}, Y_{0l}) = \{(X_{0li}, Y_{0li})\}_{i=1}^m$ of size $m = 100$ are generated from the bivariate normal distribution for each parameter set in Table 1. Using the first sample to construct the estimated MALP and LSLP,

Table 1: Parameter sets for the bivariate normal distribution, together with contour plot of the associated distributions.

	μ_X	μ_Y	σ_X	σ_Y	ρ	ρ_{XY}^c
Set 1	5	5	2	4	0.816	0.653
Set 2	8	4	3	3	0.5	0.265
Set 3	9	1	4	2	0.3	0.057



the predicted values of Y_{0l} , given X_{0l} , for the second sample are obtained, denoted by \hat{Y}_{0l}^* and \hat{Y}_{0l}^\dagger , respectively. The performances of the predictors are measured by the PCC, CCC, and MSE between Y_0 and \hat{Y}_0 :

$$\begin{aligned}\hat{\rho}_{y_0\hat{y}_0} &= \widehat{\text{PCC}}(y_0, \hat{y}_0) = \frac{S_{y_0\hat{y}_0}}{S_{y_0}S_{\hat{y}_0}}; \\ \hat{\rho}_{y_0\hat{y}_0}^c &= \widehat{\text{CCC}}(y_0, \hat{y}_0) = \frac{2S_{y_0\hat{y}_0}}{S_{y_0}^2 + S_{\hat{y}_0}^2 + (\bar{y}_0 - \bar{\hat{y}}_0)^2}; \\ \hat{\mathcal{M}}_{y_0\hat{y}_0} &= \widehat{\text{MSE}}(y_0, \hat{y}_0) = \frac{1}{\text{MReps}} \sum_{l=1}^{\text{MReps}} (y_{0l} - \hat{y}_{0l})^2.\end{aligned}\tag{18}$$

Figure 5 consists of the boxplots of the three performance measures based on $\{(Y_{0l}, \hat{Y}_{0l}^*)\}_{l=1}^{\text{MReps}}$ and $\{(Y_{0l}, \hat{Y}_{0l}^\dagger)\}_{l=1}^{\text{MReps}}$. Panel A shows the prediction performance measured by the PCC criterion, so

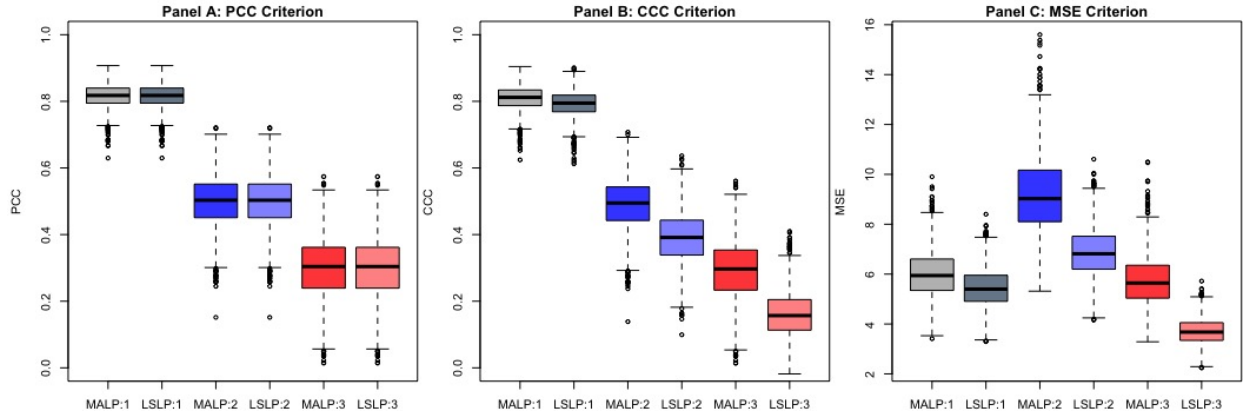


Figure 5: Comparisons on prediction performance between MALP and LSLP: the side-by-side boxplots based on 2000 empirical PCC, CCC, and MSE values between Y_0 and \hat{Y}_0 for the different parameter sets.

larger values indicate better performance. Note that the MALP has the same PCC as the LSLP for all three parameter specifications. This is an expected result since the PCC is invariant with respect to linear transformations. On the other hand, the prediction performance as measured by the CCC criterion in panel B shows some discrepancy between the MALP and the LSLP. For any parameter specification, the CCC of the MALP is higher than that of the LSLP, implying that the MALP is preferable to the LSLP with respect to the CCC criterion. Furthermore, observe that the median values of the CCC from the MALP are close to the $|\rho|$ values (0.816, 0.5, and 0.3) in the parameter set used for the data generation. Note that theoretically, $|\rho|$, which is γ since $p = 1$, is the value of the CCC if the parameters are known, but since we are using the estimated MALP, there is sampling variability in these empirical CCC values, and some of them exceed the value of $|\rho|$. Lastly, panel C shows the prediction performance measured by the MSE criterion, so smaller

values indicate better performances. Note that the MSE values vary with respect to the parameter sets, but the LSLP shows better performance than the MALP regardless of the parameter selection. The results indicate that there is no uniformly best predictor with respect to all three criteria. As such, the choice of a predictor should depend on the measure of predictive performance that one utilizes. If one is interested in the CCC criterion, the MALP would be the better choice for the predictor; whereas, if one considers the MSE criterion, the LSLP would be the better predictor.

5 Confidence and Prediction Intervals

5.1 Computational Approaches for Standard Errors

The asymptotic normality for MALP is an important property of the estimated MALP that provides an approximate method for uncertainty quantification through the expression of the asymptotic variance σ_{MA}^2 given in (14), which could be used for constructing confidence or prediction intervals. However, for general non-normal distributions, as noted earlier, the analytic derivation of an explicit expression for σ_{MA}^2 could be quite involved. An alternative computer-intensive approach for approximating the variance of the estimated MALP is via resampling approaches such as the jackknife or bootstrap procedures; see Efron and Hastie [10, Chapter 10]. The resulting approximate variances are reasonable alternatives to the asymptotic variance and may even be better for small-to-moderate sample sizes n .

For the jackknife and bootstrap approaches, suppose we observe a random sample $\{\mathbf{X}, \mathbf{Y}\} = \{(X_i, Y_i)\}_{i=1}^n$ and the estimated predictor $\hat{y}^*(x_0) = \hat{y}^*(x_0; \{\mathbf{x}, \mathbf{y}\})$ has the form in (8). For the jackknife approach, we create a sample without the j th component $\{\mathbf{X}_{(j)}, \mathbf{Y}_{(j)}\} = \{(X_1, Y_1)^\top, \dots, (X_{j-1}, Y_{j-1})^\top, (X_{j+1}, Y_{j+1})^\top, \dots, (X_n, Y_n)^\top\}^\top$. Then, the jackknife estimated predictor based on the observed sample can be defined $\hat{y}_{(j)}^*(x_0) = \hat{y}^*(x_0; \{\mathbf{x}_{(j)}, \mathbf{y}_{(j)}\})$. Lastly, we define the jackknife estimate of variance for $\hat{y}^*(x_0)$:

$$\hat{\sigma}_{\text{JK}}^2(x_0) = \frac{n-1}{n} \sum_{j=1}^n \left(\hat{y}_{(j)}^*(x_0) - \bar{y}_{\text{JK}}^*(x_0) \right)^2 \quad \text{with} \quad \bar{y}_{\text{JK}}^*(x_0) = \frac{1}{n} \sum_{j=1}^n \hat{y}_{(j)}^*(x_0). \quad (19)$$

For the bootstrap approach, we draw a bootstrap sample of size n from $\{\mathbf{X}, \mathbf{Y}\}$ with equal probability and with replacement: $\{\mathbf{X}^*, \mathbf{Y}^*\} = \{(X_1^*, Y_1^*)^\top, (X_2^*, Y_2^*)^\top, \dots, (X_n^*, Y_n^*)^\top\}^\top$. Based on this bootstrap sample, the associated individual bootstrap estimate of MALP is $\hat{y}^{**}(x_0) = \hat{y}^*(x_0; \{\mathbf{x}^*, \mathbf{y}^*\})$. Repeating this resampling procedure B times, we obtain the bootstrap replicates: $\hat{y}_1^{**}(x_0), \hat{y}_2^{**}(x_0), \dots, \hat{y}_B^{**}(x_0)$. Lastly, we define the bootstrap estimate of variance for $\hat{y}^*(x_0)$:

$$\hat{\sigma}_{\text{BS}}^2(x_0) = \frac{1}{B-1} \sum_{j=1}^B \left(\hat{y}_j^{**}(x_0) - \bar{y}_{\text{BS}}^{**}(x_0) \right)^2 \quad \text{with} \quad \bar{y}_{\text{BS}}^{**}(x_0) = \frac{1}{B} \sum_{j=1}^B \hat{y}_j^{**}(x_0). \quad (20)$$

The resulting $\hat{\sigma}_{JK}^2(x_0)$ and $\hat{\sigma}_{BS}^2(x_0)$ are the jackknife and bootstrap estimates of $\sigma_{MA}^2(x_0)/n$.

5.2 Interval Estimation of MALP

Given the asymptotic normality in (14), an asymptotic $100(1 - \alpha)\%$ confidence interval (CI) for $\tilde{Y}^*(x_0)$ would be as follows, where $z_\alpha = \Phi^{-1}(1 - \alpha)$, the $100(1 - \alpha)$ th quantile of the standard normal distribution, whose distribution and quantile functions are denoted, respectively, by $\Phi(\cdot)$ and $\Phi^{-1}(\cdot)$:

$$\Gamma[x_0, (x, y); \alpha] = \left[\hat{y}^*(x_0) \pm z_{\alpha/2} \frac{\sigma_{MA}(x_0)}{\sqrt{n}} \right].$$

Note that the standard error term $\frac{\sigma_{MA}(x_0)}{\sqrt{n}}$ is unknown. The first three CIs are obtained when this standard error is estimated by the asymptotic standard error obtained in (15), jackknife standard deviation obtained in (19), and the bootstrap standard deviation obtained in (20). We denote these CIs by $\Gamma_1[x_0, (x, y); \alpha]$, $\Gamma_2[x_0, (x, y); \alpha]$, and $\Gamma_3[x_0, (x, y); \alpha]$, respectively. An alternative option for the construction of CIs for MALP is a fully nonparametric approach based on resampling procedures. We adopt some of these approaches for our illustration: the bootstrap- t CI procedure, $\Gamma_4[x_0, (x, y); \alpha]$; the standard bootstrap percentile CI procedure, $\Gamma_5[x_0, (x, y); \alpha]$; and the bias-corrected accelerated percentile CI procedure, $\Gamma_6[x_0, (x, y); \alpha]$. For forms and details of these CIs, see Section 3 in the Appendix. See also Davison and Hinkley [8, Chapter 5] and Efron and Hastie [10, Chapter 11] for the constructions and discussions regarding the resampling-based CI procedures.

For comparison of these procedures, we provide simulation results for the case of $p = 2$. The set of parameters of the simulation coincides with the first experiment with $\gamma = 0.5$ in Section 4.1, so the results could be understood in light of Figures 9 and 10. The prediction point was randomly chosen to be at $(x_1, x_2) = (3.177, 6.457)$ whose squared Mahalanobis distance from the mean is 5.071. For a confidence level $1 - \alpha = 0.95$, we performed simulations with sample sizes $n \in \{50, 100, 200\}$ for the CI procedures, and their empirical coverage probabilities and average lengths were computed based on 10000 simulation replications. For the bootstrap-based CIs, we utilize 2000 resamplings and 30 sub-resamplings.

The empirical coverage probabilities and average lengths standardized by the sample size are summarized in Table 2 with the corresponding standard errors. In terms of coverage probability, Γ_2 and Γ_3 show satisfactory results for all three sample sizes. In contrast, Γ_4 , Γ_5 , and Γ_6 have lower coverage rates relative to what is desired, although these rates improve as the sample size is increased. Lastly, Γ_1 shows less coverage rate than desired for $n = 50$, but becomes satisfactory when $n = 100$ and $n = 200$ as the empirical coverage probabilities are consistent with the desired level 0.95. With regards to the standardized average length, Γ_1 consistently shows good performance by having a shorter average length. This becomes more pronounced when $n = 100$ and $n = 200$ since it also then possesses the desired coverage rate. Γ_2 and Γ_3 have stable performances, providing moderate expected lengths. On the other hand, those of Γ_5 and Γ_6 have low coverage rates when

Table 2: Performance of the different CIs: in panel A, the empirical coverage probabilities for the CIs with the standard errors; and, in panel B, the average standardized (multiplied by \sqrt{n}) lengths for the CIs with the standard errors. The CI procedures are constructed for 0.95 nominal level and the performance measures are calculated based on 10000 replications.

Panel A	n	Γ_1 : Asymp.	Γ_2 : Jack	Γ_3 : Boot	Γ_4 : Boot-t	Γ_5 : Percentile	Γ_6 : BCa	
Coverage Probability (Standard Error)	50	0.943 (.0023)	0.948 (.0022)	0.947 (.0022)	0.937 (.0024)	0.941 (.0024)	0.932 (.0025)	
	100	0.946 (.0023)	0.948 (.0022)	0.946 (.0023)	0.942 (.0023)	0.943 (.0023)	0.938 (.0024)	
	200	0.95 (.0022)	0.95 (.0022)	0.948 (.0022)	0.946 (.0023)	0.949 (.0022)	0.945 (.0023)	
	Panel B	n	Γ_1 : Asymp.	Γ_2 : Jack	Γ_3 : Boot	Γ_4 : Boot-t	Γ_5 : Percentile	Γ_6 : BCa
	Average Length (Standard Error)	50	17.042 (.0564)	18.221 (.0672)	18.384 (.0651)	18.272 (.069)	18.539 (.0641)	18.092 (.0573)
		100	16.716 (.0347)	17.221 (.039)	17.131 (.0399)	17.147 (.0418)	17.275 (.0389)	17.182 (.0377)
200		16.563 (.023)	16.813 (.0262)	16.697 (.0272)	16.849 (.0292)	16.812 (.0259)	16.780 (.0257)	

n is small, which contributed to their having moderately shorter average lengths. Finally, Γ_4 exhibited the worst performance when $n = 200$, providing the largest average length; additionally, the relatively moderate lengths observed when $n = 50$ and $n = 100$ may not be fully meaningful since they may be explained by the unsatisfactory coverage rates.

5.3 Prediction Intervals for $Y(x_0)$

While the confidence interval provides an estimate together with a measure of uncertainty for the true MALP, in practical settings we may be more interested in predicting the value of a new observation Y at $X = x_0$ together with a measure of uncertainty regarding the prediction. In this subsection, we therefore consider this problem of constructing a prediction interval (PI) for the new observation $Y(x_0)$ based on the MALP.

Theorem 3. *Suppose (X, Y) follows a multivariate normal distribution with non-singular Σ and $\Sigma_{YX} \neq 0$. Then, the $100(1 - \alpha)\%$ prediction interval for $Y(x_0)$ based on MALP becomes:*

$$\left[(\hat{Y}^*(x_0) + \hat{b}(x_0)) \pm z_{\alpha/2} S_Y \sqrt{1 - \hat{\gamma}^2} \sqrt{1 + \frac{1}{n} \hat{D}_{MA}^2(x_0)} \right], \quad (21)$$

where $\hat{D}_{MA}^2(x_0) = \frac{2}{1 + \hat{\gamma}} + \frac{1}{\hat{\gamma}^2} (x_0 - \bar{X}) S_{XX}^{-1} (x_0 - \bar{X})^\top - \left[\frac{(1 - \hat{\gamma}^2)}{S_Y^2 \hat{\gamma}^4} \right] [(x_0 - \bar{X}) S_{XX}^{-1} S_{XY}]^2$.

Proof. See Section 1.3 in the Appendix. □

Note that $\hat{Y}^*(x_0) + \hat{b}(x_0) = \hat{Y}^\dagger(x_0)$, and the PI in (21) tends to be wider compared to the PI

based on the LSLP:

$$\left[\hat{Y}^\dagger(x_0) \pm z_{\alpha/2} S_Y \sqrt{(1 - \hat{\gamma}^2)} \sqrt{1 + \frac{1}{n} [1 + (x_0 - \bar{X}) S_{XX}^{-1} (x_0 - \bar{X})^\top]} \right], \quad (22)$$

indicating the larger variability accruing with the MALP relative to the LSLP. For small to moderate n , when the asymptotic approximations may not be adequate, the prediction intervals based on the LSLP and the MALP may be improved by estimating the standard error $\sigma_{LS}(x_0)/\sqrt{n}$ and $\sigma_{MA}(x_0)/\sqrt{n}$ and the bias $b(x_0)$ through computational approaches such as the jackknife or the bootstrap methods described in Section 5.1.

6 Illustrative Data Analyses

In this section, we demonstrate the prediction procedures using two real data sets. The R programs that implement the prediction procedures, as well as those used for performing the simulation or computer experiment studies in this paper, are in the publicly accessible R package, called the `malp` package (Chausse et al. [5]). The first data set, with $n = 46$, pertains to eye measurements used in Abedi et al. [1]. This is a simple case in that there is only one predictor variable, so $p = 1$. The second data set contains body fat data with $n = 252$ and with more than one predictor variable, so $p > 1$.

6.1 Eye Data Set

In ophthalmology, central subfield macular thickness (CSMT) measurements can be obtained by optical coherence tomography (OCT). As introduced in Figure 1, Abedi et al. [1] focused on two types of OCT: time-domain Stratus OCT, the most widely used method prior to 2006; and spectral-domain Cirrus OCT, a more advanced method. As Cirrus OCT replaces Stratus OCT, the agreement between the measurements from the two methods is of interest to researchers in the field. For this purpose, Abedi et al. [1] provided a CCC-based conversion function from the Cirrus OCT measurement to the Stratus OCT measurement.

In the data set, both OCTs were measured from 46 subjects, i.e., 92 eyes, but only 61% of these observations were selected based on the reliability of the OCTs (signal strength ≥ 6 for both approaches). The computed correlations are $\hat{\rho} = 0.783$ and $\hat{\rho}^c = 0.200$. Based on the data set, two conversion formulas were introduced: i) $x \mapsto x_1 = x - 60$ was based on a location shift which adjusts for the mean difference between Cirrus and Stratus OCTs, and this leads to $\hat{\rho}_{x_1y}^c = 0.756$; ii) $x \mapsto x_2 = 0.76x - 0.51$ was chosen to maximize the CCC, yielding $\hat{\rho}_{x_2y}^c = 0.781$; see Abedi et al. [1, Figure 2].

From a prediction perspective, we follow Abedi et al. [1]’s idea of obtaining the Stratus OCT using the Cirrus OCT. We start with an *illustrative* case using a plug-in approach: $\hat{y}^*(x_0) =$

$\hat{\mu}_y + \text{Sgn}\{\hat{\rho}\}(\hat{\sigma}_Y/\hat{\sigma}_X)(x_0 - \hat{\mu}_x)$ and $\hat{y}^\dagger(x_0) = \hat{\mu}_y + \hat{\rho}(\hat{\sigma}_Y/\hat{\sigma}_X)(x_0 - \hat{\mu}_x)$. We consider the OS (left eye) and the OD (right eye) measurements separately in order to mitigate the impact of their correlation ($n_{\text{OS}} = 26$ and $n_{\text{OD}} = 30$). The predicted values from these predictors, together with the observed values, are then plotted in Figure 6.

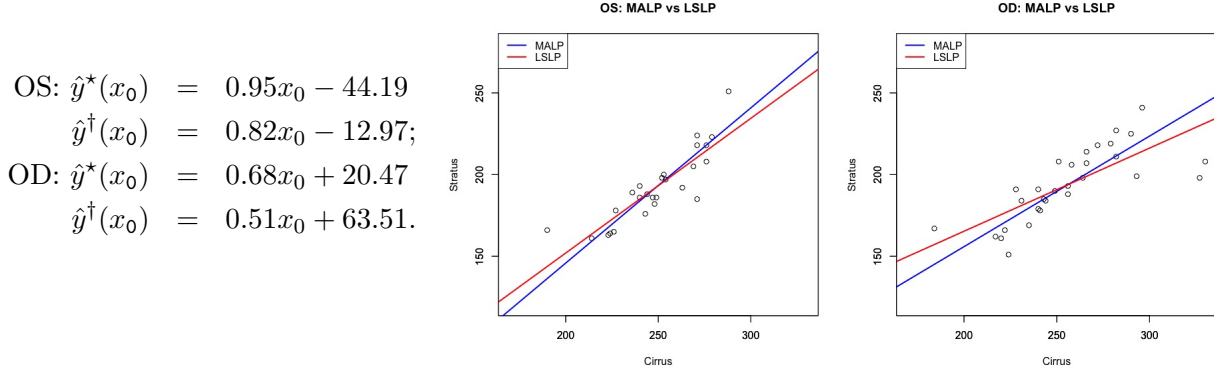


Figure 6: The comparison between the estimated MALP and the estimated LSLP for Stratus OCT based on Cirrus OCT: OS (left eye) and OD (right eye) are presented separately.

Using the observed values and the predicted values, we computed the PCC, CCC, and MSE, and these are summarized in the second main column labeled ‘Illustrative Case’ in Table 3. Note, however, that we are using the observed data twice: for the construction of the predictors and then for the evaluation of their performance, hence such comparisons could be biased due to data double-dipping. To obtain a more appropriate evaluation of the performance and comparison,

Table 3: Prediction performances of MALP and LSLP measured by PCC, CCC, and MSE.

Prediction	Illustrative Case				Realistic Case			
	OS (Left Eye)		OD (Right Eye)		OS (Left Eye)		OD (Right Eye)	
Predictor	MALP	LSLP	MALP	LSLP	MALP	LSLP	MALP	LSLP
PCC	0.868	0.868	0.752	0.752	0.601	0.601	0.667	0.667
CCC	0.868	0.859	0.752	0.722	0.560	0.466	0.614	0.556
MSE	122.735	114.636	228.977	200.573	488.458	406.421	343.476	277.980

which circumvents the data double-dipping, of $\hat{y}^*(x_0)$ and $\hat{y}^\dagger(x_0)$ using this eye data, we utilize a resampling approach. We randomly split the data in half into training and testing sets so that the training set is used for constructing the estimated MALP and the estimated LSLP, respectively. The test set is used for evaluating their performance, where the predictions from the predictors using the Cirrus OCT values are compared to the observed Stratus OCT values. This process is repeated $N_{\text{reps}} = 2000$ times. For the resulting 2000 values of the PCC, CCC, and MSE, we then obtain their respective means. The results are summarized in the third main column labeled ‘Realistic Case’ in Table 3.

The results in Table 3 indicate that the MALP performs better than LSLP when the criterion is the CCC, but the situation is reversed when the criterion is the MSE. Thus, as noted earlier in the computer experiments section, it behooves for the researcher to decide first what desirable property the predictor should have prior to its choice: i) if the goal is to maximize agreement, then the MALP is preferable; while ii) if the goal is to minimize the MSE, then the LSLP is preferable.

To obtain a comparable conversion formula with that of Abedi et al. [1], we then combined the OD and OS observations, though it should be noted that this is a violation of the independence assumption since it is expected that the left and right eye measurements will be correlated. Using our procedure, we obtained the conversion function given in the first equation in Figure 7, and we also provide the conversion function of Abedi et al. [1], which is the second equation in the same figure. Observe that the two prediction functions (lines) depicted in the plot in Figure 7 are almost identical. The slight discrepancy is that the equation of Abedi et al. [1] was obtained through

Conversion Formulae

$$\hat{y}^*(x_0) = 0.765x_0 - 0.341;$$

$$\hat{y}_{\text{Abedi}}(x_0) = 0.760x_0 - 0.510.$$

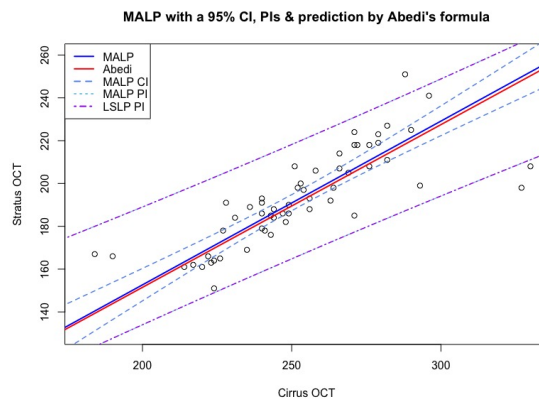


Figure 7: Scatter plots of two OCTs superimposed with the estimated prediction lines based on two conversion formulae: the estimated MALP and Abedi’s conversion formula. Also included are the 95% asymptotic CI for the MALP and the 95% asymptotic prediction intervals based on the LSLP and the MALP.

a grid search, while our procedure was obtained from an analytical derivation, hence it is more accurate. In fact, the CCC of the observed and predicted values from the two equations, which are both about 0.783, differed by less than 10^{-5} , with the one from our conversion equation just a tad higher. In addition, the 95% asymptotic normal confidence interval for MALP is presented around the estimated MALP, as well as the prediction intervals based on the formulas in (22) and (21). Observe that the two prediction interval curves are not so different owing to the fact that $\hat{\gamma} = 0.783$. In addition, note that the prediction interval curves are not centered on the estimated MALP line, rather they are centered on the estimated LSLP line as previously shown, though this line is not depicted in the plot for simplicity.

6.2 Body fat Data Set

The percent body fat is an important bodily characteristic that serves as a marker for the health status of an individual. Being able to infer its value from easily-measured or determined bodily characteristics, such as age, weight, height, circumference measurements, or skin-fold measurements is therefore of interest, e.g., Behnke and Wilmore [3], Katch and McArdle [16]. For example, one could obtain the percent body fat from body density via underwater weighting based on Siri's equation $100 \times \text{Body fat} = 495/\text{Body Density} - 450$ as in Siri [28]. Including body density (BD) and percent body fat (PBF), the data set of interest contains 13 additional variables such as age (in years), weight (WGT, in pounds), height (HGT, in inches); several body circumference measurements (in cm): neck (NCK), chest (CST), abdomen (ABD), hip, thigh (TGH), knee (KN), ankle (ANK), biceps (BCP), forearm (FA), and wrist (WRT) for 252 men. The data set was originally in Penrose et al. [25] and became available to the public by courtesy of Dr. A. Garth Fisher.

Using the data set, our goal is to provide an illustration of the MALP procedure to predict the percent body fat based on other easily-measured or determined body characteristics. While there are several variables that have high correlations with the percent body fat variable, some of those are highly correlated with each other, e.g., see Table 7 in Section 4 of the Appendix. Using the exhaustive search method based on LSLP, we selected the subsets of variables that yielded the largest R^2 for the specified subset sizes of 1, 2, 4, 6, and 8. For each of these subsets of predictor variables, we obtained the estimated MALP and estimated LSLP functions, and calculated the percent body fat predicted values from each predictor for all $n = 252$ subjects. Thus, note immediately that we are double-dipping on the data in that we used it to construct the predictors, and then used the data again to obtain the predicted values. Table 4 contains the coefficients of these linear predictors for each of the subsets, together with their associated performance measures given by the PCC, CCC, and MSE, calculated using the observed and predicted values of the percent body fat variable. Figure 8 presents these performance values of the MALP and LSLP pictorially. As expected from classical multiple linear regression theory, the PCC of the LSLP, which is also the PCC of the MALP from an earlier result, equals the multiple correlation coefficient, as could be seen from Table 4. In addition, observe that as the subset of predictor variables used in the model increases in size, the performance of the predictors also improves, though there is a diminishing rate of improvement as could be seen from Figure 8. However, as we point out in the Concluding Remarks section, these measures need to be adjusted for the number of predictor variables used, akin to the adjusted- R^2 in classical multiple linear regression, if a proper comparison of performance of prediction functions with a different number of predictor variables is to be done. This issue remains an open research problem.

Lastly, the panels in Figure 16 in the Appendix show the scatter plots of the pairs of observed and predicted values from each of the fitted prediction functions. Looking at the scatter plots, for

Table 4: Coefficients of the MALP and LSLP with the body fat variable as a dependent variable for different subsets of predictor variables, together with their corresponding performance measures computed on the whole data set.

Subset	Coefficients of the Linear Predictors									
	A		B		C		D		E	
Predictor	MALP	LSLP	MALP	LSLP	MALP	LSLP	MALP	LSLP	MALP	LSLP
Intercept	-52.68	-39.28	-57.64	-45.95	-43.84	-34.85	-47.62	-38.32	-29.24	-22.66
ABD	0.776	0.631	1.167	0.990	1.161	0.996	1.059	0.912	1.093	0.945
WGT			-0.175	-0.148	-0.158	-0.136	-0.159	-0.136	-0.104	-0.090
FA					0.552	0.473	0.568	0.489	0.597	0.516
WRT					-1.756	-1.506	-2.067	-1.779	-1.778	-1.537
AGE	-	-					0.073	0.063	0.076	0.066
TGH							0.256	0.220	0.350	0.302
NCK									-0.540	-0.467
HIP							-	-	-0.226	-0.195
PCC	0.813	0.813	0.848	0.848	0.857	0.857	0.861	0.861	0.864	0.864
CCC	0.813	0.796	0.848	0.836	0.857	0.847	0.861	0.851	0.864	0.855
MSE	26.029	23.601	21.232	19.616	19.905	18.485	19.421	18.070	18.969	17.680

both the MALP and the LSLP, the point clouds appear to cluster around the 45° line, with those for the MALP tending to be a tad more closely clustered to this line than those for the LSLP, which is to be expected from its development since it is focused towards achieving a higher agreement between predicted and predictand values. But note also that there is more variability in the MALP predictions compared to the LSLP predictions, which is the price one pays by trying to achieve a higher degree of agreement, consistent with the universal adage that *there is no free lunch!*

7 Concluding Remarks

In this study, we investigated a new predictor, called the MALP, which is designed to maximize the agreement between the predictor and predictand as measured by the CCC. For the case with a single-dimensional covariate or feature, the predictor function coincides with those derived through other approaches, such as the geometric mean regression or the least-triangle regression. However, the development of our MALP allows an extension to the case with multi-dimensional covariates or features, which may not be possible or easy to achieve with the other approaches relying on geometric motivations. In addition, the MALP has a computational profile that is of the same order as the least-squares linear predictor (LSLP) since it is obtainable as a linear transformation of the LSLP with coefficients depending on the multiple correlation coefficient.

Distributional properties of the MALP were obtained, with the asymptotic normality justified using the U -statistics approach, and with a closed-form of the asymptotic variance obtained under a multivariate normal model. Computer experiments showed that the quality of the normal approximation and the approximations of asymptotic mean and variance are quite satisfactory when

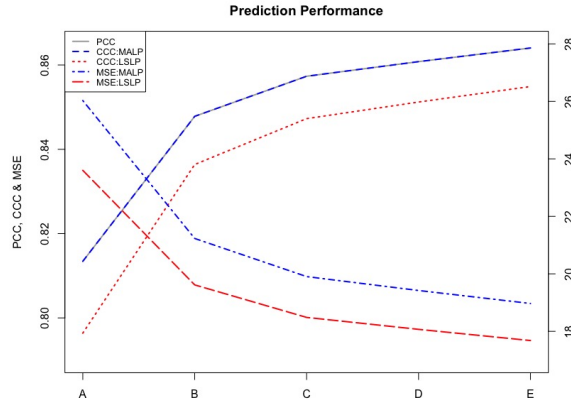


Figure 8: Plots of the performance measures (PCC, CCC, and MSE) of the MALP and LSLP for the body fat data as the size of subsets of predictors in the model increases. Note that the PCC and CCC of the MALP coincide.

the multiple correlation coefficient is not too close to zero and the sample size is at least moderate. It was also demonstrated via the simulation studies for a few sets of parameter values under normality that the interval estimators for the MALP are satisfactory. The MALP-based prediction procedures were also demonstrated using two real data sets: an eye data set and a body fat data set.

Comparisons between MALP and LSLP were also performed. The MALP and LSLP belong to the class of linear predictors that maximize the PCC between the predictor and the predictand, with the MALP uniquely maximizing the CCC, whereas the LSLP is uniquely minimizing the MSE. Whether one should prefer the LSLP over the MALP, or the MALP over the LSLP, depends on the performance measure that is desired for the predictor. Thus, if one is seeking a linear predictor that will have a high CCC with what is being predicted, then the MALP should be preferred; while if the MSE is the desired criterion, then the LSLP is the preferred prediction function.

We conclude by pointing out some open research problems related to the maximum agreement predictor. First, when comparing the performance of MALPs with different sets of predictor variables, simply computing their CCCs could be a misleading comparison measure since they are not adjusted for the number of predictor variables being used, cf., in the illustrative example using the body fat data set. So an important question is how could the CCC be properly adjusted to account for the number of predictor variables, akin to the adjusted- R^2 in classical multiple linear regression? Second, there is the problem of developing hypothesis tests and confidence intervals for the coefficients of the MALP. Are there analogous procedures to the inferential procedures in classical multiple linear regression? Third, when there are many potential predictor variables or features, how could the MALP approach be utilized for variable selection? This may require a

resolution of the first problem described above. Another avenue of investigation is to incorporate a regularization component in the MALP derivation, leading to a so-called *regularized* MALP.

Acknowledgements

We are very grateful to Dr. Gelareh Abedi for providing and letting us utilize the eye data set in the illustration section and in the R package `malp`.

Disclaimer

E. Peña was Program Director in the Division of Mathematical Sciences at the National Science Foundation (NSF). He received support (NSF Grant 2049691) for research, which included work on this manuscript. Any opinions, findings, conclusions, or recommendations expressed in this material are those of the authors and do not necessarily reflect the views of NSF.

R-package `malp`

The R-package `malp` implements the maximum agreement linear prediction and provides the two data sets which are used in the paper. A vignette that describes how to use the different functions is also included in the package. It is available online on the development page <https://github.com/pchause/malp>. To install the package in R, install and load the package `devtools` and run the command `install_github("pchause/malp")`.

References

- [1] Gelareh Abedi, Payal Patal, Gheorghe Doros, and Manju L Subramanian. Transitioning from stratus OCT to cirrus OCT: A comparison and a proposed equation to convert central sub-field macular thickness measurements in healthy subjects. *Graefe's Archive for Clinical and Experimental Ophthalmology*, 249(9):1353–1357, 2011.
- [2] F Barker, YC Soh, and RJ Evans. Properties of the geometric mean functional relationship. *Biometrics*, 44:279–281, 1988.
- [3] Albert Richard Behnke and Jack H Wilmore. *Evaluation and regulation of body build and composition*. Prentice Hall, Englewood Cliffs, NJ, 1974.
- [4] Matteo Bottai, Taeho Kim, Benjamin Lieberman, George Luta, and Edsel A. Peña. On optimal correlation-based prediction. *The American Statistician*, 76:313–321, 2022.
- [5] Pierre Chausse, Taeho Kim, and Edsel A. Peña. *malp: Maximum Agreement Linear Prediction*, 2023. URL <https://github.com/pchause/malp>. R package version 0.1-0.

- [6] Ronald Christensen. Comment on “On optimal correlation-based prediction,” by Bottai et al.(2022). *The American Statistician*, 76(4):322–322, 2022.
- [7] Noel Cressie. *Statistics for spatial data*. John Wiley & Sons, Hoboken, NJ, 2015.
- [8] Anthony Christopher Davison and David Victor Hinkley. *Bootstrap methods and their application*. Number 1. Cambridge University Press, Cambridge, 1997.
- [9] Norman R Draper and Yonghong Fred Yang. Generalization of the geometric mean functional relationship. *Computational Statistics & Data Analysis*, 23(3):355–372, 1997.
- [10] Bradley Efron and Trevor Hastie. *Computer age statistical inference*. Cambridge University Press, New York, NY, 2016.
- [11] Peter M Fayers and Ron D Hays. Should linking replace regression when mapping from profile-based measures to preference-based measures? *Value in Health*, 17(2):261–265, 2014.
- [12] Francis Galton. I. Co-relations and their measurement, chiefly from anthropometric data. *Proceedings of the Royal Society of London*, 45(273-279):135–145, 1889.
- [13] Malay Ghosh. Constrained Bayes estimation with applications. *Journal of the American Statistical Association*, 87(418):533–540, 1992.
- [14] Wassily Hoeffding. A Class of Statistics with Asymptotically Normal Distribution. *The Annals of Mathematical Statistics*, 19(3):293 – 325, 1948.
- [15] Leon Isserlis. On a formula for the product-moment coefficient of any order of a normal frequency distribution in any number of variables. *Biometrika*, 12(1/2):134–139, 1918.
- [16] Frank I Katch and William D McArdle. *Nutrition, weight control, and exercise*. Houghton Mifflin Company, Boston, MA, 1977.
- [17] KA Kermack and John BS Haldane. Organic correlation and allometry. *Biometrika*, 37(1/2): 30–41, 1950.
- [18] Tonya S King and Vernon M Chinchilli. Robust estimators of the concordance correlation coefficient. *Journal of Biopharmaceutical Statistics*, 11(3):83–105, 2001.
- [19] Joseph Lee Rodgers and W Alan Nicewander. Thirteen ways to look at the correlation coefficient. *The American Statistician*, 42(1):59–66, 1988.
- [20] Lawrence Lin. A concordance correlation coefficient to evaluate reproducibility. *Biometrics*, 45:255–268, 1989.
- [21] Lawrence Lin. Assay validation using the concordance correlation coefficient. *Biometrics*, 48: 599–604, 1992.
- [22] Lawrence Lin, AS Hedayat, Bikas Sinha, and Min Yang. Statistical methods in assessing agreement: Models, issues, and tools. *Journal of the American Statistical Association*, 97 (457):257–270, 2002.
- [23] Lawrence Lin, AS Hedayat, and Wenting Wu. *Statistical tools for measuring agreement*. Springer, New York, 2012.

- [24] Karl Pearson. Mathematical contributions to the theory of evolution. iii. Regression, heredity and panmixia. *Philosophical Transactions of the Royal Society A*, 187:253–318, 1896.
- [25] Keith W Penrose, AG Nelson, and AG Fisher. Generalized body composition prediction equation for men using simple measurement techniques. *Medicine & Science in Sports & Exercise*, 17(2):189, 1985. URL <http://lib.stat.cmu.edu/datasets/bodyfat>.
- [26] Alvin C Rencher and G Bruce Schaalje. *Linear models in statistics*. John Wiley & Sons, 2008.
- [27] Robert J Serfling. *Approximation theorems of mathematical statistics*. Wiley, New York, 1980.
- [28] William E Siri. The gross composition of the body. In *Advances in Biological and Medical Physics*, volume 4, pages 239–280. Elsevier, 1956.
- [29] Richard J Smith. Use and misuse of the reduced major axis for line-fitting. *American Journal of Physical Anthropology: The Official Publication of the American Association of Physical Anthropologists*, 140(3):476–486, 2009.
- [30] Stephen M Stigler. Francis Galton’s account of the invention of correlation. *Statistical Science*, 4:73–79, 1989.

Appendices

This appendix consists of the proofs of theorems in section A, additional results of the computer experiments in section B, the forms of confidence interval procedures in section C, and the description of the body fat data set in section D.

Appendix A Proofs

In this section, we provide proofs of Theorem 1, Theorem 2, and Theorem 3.

A.1 Proof of Theorem 1

Proof. Consider the class of linear predictors \mathcal{H}_{LP} . We seek an element $\tilde{Y}^*(\cdot) \in \mathcal{H}_{\text{LP}}$ such that $\rho_{\tilde{Y}^*}^c := \rho^c(Y, \tilde{Y}^*(X)) = \sup_{\{\tilde{Y} \in \mathcal{H}_{\text{LP}}\}} \rho^c(Y, \tilde{Y}(X))$. Under the linearity condition, the moments for the MALP can be expressed in the following concrete forms:

$$\mu_{\tilde{Y}} = \alpha + \mu_X \beta, \quad \sigma_{\tilde{Y}}^2 = \beta^T \Sigma_{\text{XX}} \beta, \quad \text{and} \quad \sigma_{Y\tilde{Y}} = \Sigma_{\text{YX}} \beta.$$

Then, the CCC between the linear predictor and the predictand becomes:

$$\rho_{\tilde{Y}}^c = \rho^c(Y, \tilde{Y}(X)) = \frac{2\Sigma_{\text{YX}}\beta}{\sigma_{\tilde{Y}}^2 + \beta^T \Sigma_{\text{XX}} \beta + (\mu_Y - \alpha - \mu_X \beta)^2} \tag{23}$$

from the definition of CCC. First, we can maximize $\rho_{\tilde{Y}\tilde{Y}}^c$ by taking $\alpha^* = \mu_Y - \mu_X\beta$ for any given β . In such a case, the form of CCC in (23) is simplified:

$$\rho_{\tilde{Y}\tilde{Y}}^c = \frac{2\Sigma_{YX}\beta}{\sigma_Y^2 + \beta^T\Sigma_{XX}\beta}. \quad (24)$$

By taking the logarithm on both sides, the equation becomes

$$\log \rho_{\tilde{Y}\tilde{Y}}^c = \log(2\Sigma_{YX}\beta) - \log(\sigma_Y^2 + \beta^T\Sigma_{XX}\beta).$$

To optimize with respect to β , we obtain the gradient and equate it to zero:

$$\nabla_{\beta} \log \rho_{\tilde{Y}\tilde{Y}}^c = \frac{\Sigma_{XY}}{\Sigma_{YX}\beta} - \frac{2\Sigma_{XX}\beta}{\sigma_Y^2 + \beta^T\Sigma_{XX}\beta} \stackrel{\text{set}}{=} 0.$$

Multiplying by β^T , we obtain

$$1 = \frac{2\beta^T\Sigma_{XX}\beta}{\sigma_Y^2 + \beta^T\Sigma_{XX}\beta}$$

so that

$$\sigma_Y^2 = \beta^T\Sigma_{XX}\beta. \quad (25)$$

Replacing $\beta^T\Sigma_{XX}\beta$ by σ_Y^2 in (24), the maximal $\rho_{\tilde{Y}\tilde{Y}}^c$ is of form

$$\rho_{\tilde{Y}\tilde{Y}}^c = \frac{\Sigma_{YX}\beta}{\sigma_Y^2}. \quad (26)$$

Now, we need to maximize with respect to β subject to the condition (25). Set the Lagrange equation as follows:

$$\mathcal{L}(\beta, \lambda) = \Sigma_{YX}\beta + \lambda(\beta^T\Sigma_{XX}\beta - \sigma_Y^2).$$

Obtaining the gradient for β and λ and equating it to zero

$$\nabla_{\beta}\mathcal{L}(\beta, \lambda) = \Sigma_{XY} + \lambda 2\Sigma_{XX}\beta \stackrel{\text{set}}{=} 0 \text{ and } \nabla_{\lambda}\mathcal{L}(\beta, \lambda) = \beta^T\Sigma_{XX}\beta - \sigma_Y^2 \stackrel{\text{set}}{=} 0,$$

we have the following equation:

$$\beta = -\frac{\Sigma_{XX}^{-1}\Sigma_{XY}}{2\lambda}. \quad (27)$$

The constraint in (25) then becomes

$$\sigma_Y^2 = \left(-\frac{\Sigma_{YX}\Sigma_{XX}^{-1}}{2\lambda}\right)\Sigma_{XX}\left(-\frac{\Sigma_{XX}^{-1}\Sigma_{XY}}{2\lambda}\right) = \frac{\Sigma_{YX}\Sigma_{XX}^{-1}\Sigma_{XY}}{(2\lambda)^2}.$$

Therefore,

$$2\lambda = \pm \sqrt{\frac{\Sigma_{YX}\Sigma_{XX}^{-1}\Sigma_{XY}}{\sigma_Y^2}}. \quad (28)$$

In order to choose the sign of λ , note that it must be $\Sigma_{YX}\beta \geq 0$ in (26) to maximize $\rho_{\tilde{Y}\tilde{Y}}^c$. Then,

$$\rho_{\tilde{Y}\tilde{Y}}^c = \frac{\Sigma_{YX}\beta}{\sigma_Y^2} = \frac{\Sigma_{YX} \left(-\frac{\Sigma_{XX}^{-1}\Sigma_{XY}}{2\lambda} \right)}{\sigma_Y^2} = \left(-\frac{1}{2\lambda} \right) \frac{\Sigma_{YX}\Sigma_{XX}^{-1}\Sigma_{XY}}{\sigma_Y^2}. \quad (29)$$

Thus, it has to be $2\lambda < 0$ in (28), so that the optimal α^* and β^* can be obtained as desired from (27):

$$\beta^* = \frac{\sigma_Y \Sigma_{XX}^{-1} \Sigma_{XY}}{\sqrt{\Sigma_{YX} \Sigma_{XX}^{-1} \Sigma_{XY}}} \quad \text{and} \quad \alpha^* = \mu_Y - \mu_X \beta^*.$$

The resulting MALP is $\tilde{Y}^*(X) = \alpha^* + X\beta^*$ with α^* and β^* given above. Lastly, the maximum CCC can be obtained from (29):

$$\rho_{\tilde{Y}\tilde{Y}^*}^c = \frac{(\Sigma_{YX}\Sigma_{XX}^{-1}\Sigma_{XY})/\sigma_Y^2}{\sqrt{(\Sigma_{YX}\Sigma_{XX}^{-1}\Sigma_{XY})/\sigma_Y}} = \frac{\sqrt{\Sigma_{YX}\Sigma_{XX}^{-1}\Sigma_{XY}}}{\sigma_Y} = \gamma. \quad (30)$$

To show uniqueness of the MALP, suppose we have two MALPs, $\tilde{Y}_1^*(x) = \alpha^* + x\beta^*$ and $\tilde{Y}_2^*(x) = \alpha^{**} + x\beta^{**}$. Then, we have the following relations from the first part of Remark 1-iii in the paper:

$$\rho_{\tilde{Y}\tilde{Y}_1^*}^c \leq \rho_{\tilde{Y}\tilde{Y}_1^*} \leq \gamma \quad \text{and} \quad \rho_{\tilde{Y}\tilde{Y}_2^*}^c \leq \rho_{\tilde{Y}\tilde{Y}_2^*} \leq \gamma.$$

In addition, due to the result in (30), the following equalities hold:

$$\rho_{\tilde{Y}\tilde{Y}_1^*}^c = \rho_{\tilde{Y}\tilde{Y}_2^*}^c = \rho_{\tilde{Y}\tilde{Y}_1^*} = \rho_{\tilde{Y}\tilde{Y}_2^*} = \gamma.$$

Now, from the second part of Remark 1-iii, the above equalities hold when $E[\tilde{Y}_1^*(X)] = E[\tilde{Y}_2^*(X)] = E[Y]$ and $\text{Var}[\tilde{Y}_1^*(X)] = \text{Var}[\tilde{Y}_2^*(X)] = \text{Var}[Y]$. However, the only possible case in order for these conditions to hold is when $\alpha^* = \alpha^{**}$ and $\beta^* = \beta^{**}$, thereby completing the proof of the uniqueness of the MALP. \square

A.2 Proof of Theorem 2

Proof. First, we gather known results that will be invoked in portions of the proof. For notation, $N_p(\mu, \Sigma)$ is a p -dimensional multivariate normal distribution with mean vector μ and covariance matrix Σ .

(R1) If Z_1, \dots, Z_n are independent random variables with $Z_i \sim N(\mu_i, 1)$, then $\sum_{i=1}^n Z_i^2 \sim \chi_n^2(\lambda =$

$\frac{1}{2} \sum_{i=1}^n \mu_i^2$), a chi-square distribution with degrees-of-freedom n and non-centrality parameter λ .

- (R2) If $S \sim \chi_n^2(\lambda)$, then $E(S) = n + 2\lambda$ and $\text{Var}(S) = 2n + 8\lambda$ [26, Thm 5.3b].
- (R3) If Z_1, \dots, Z_n are independent and identically distributed (IID) random p -dimensional row vectors from a $N_p(0, \Sigma)$, then the $p \times p$ random matrix $M = \sum_{i=1}^n Z_i^T Z_i \sim \mathcal{W}_p(n, \Sigma)$, a p -dimensional Wishart distribution. In such a case, $E(M) = \Sigma$ and $\text{Var}(M_{ij}) = n(\sigma_{ij}^2 + \sigma_{ii}\sigma_{jj})$ with $\Sigma = [(\sigma_{ij})]$ for $i, j = 1, 2, \dots, p$.
- (R4) A $p \times p$ random matrix M^{-1} has a p -dimensional inverse Wishart distribution with parameters (n, Σ^{-1}) , denoted $M^{-1} \sim \mathcal{W}_p^{-1}(n, \Sigma^{-1})$, if $M \sim \mathcal{W}_p(n, \Sigma)$. In such a case, $E(M^{-1}) = \Sigma^{-1}/(n - p - 1)$ for $n > p + 1$.
- (R5) If Y is an $n \times 1$ random vector with $Y \sim N_n(\mu, \Sigma)$ where Σ is nonsingular, then, for an $n \times n$ symmetric matrix A of constants with rank r , $Q = Y^T A Y \sim \chi_r^2(\lambda = \frac{1}{2} \mu^T A \mu)$ if and only if $A\Sigma$ is idempotent [26, Thm 5.5].
- (R6) If $Y \sim N_n(\mu, \Sigma)$, B is a $k \times n$ matrix of constants and A is an $n \times n$ symmetric matrix of constants, then BY and $Y^T A Y$ are independent if and only if $B\Sigma A = 0$ [26, Thm 5.6a].
- (R7) If $Y \sim N_n(\mu, \Sigma)$ and A and B are $n \times n$ symmetric matrices of constants, then $Y^T A Y$ and $Y^T B Y$ are independent if and only if $A\Sigma B = 0$ [26, Thm 5.6b].
- (R8) If (X, Y) is a $1 \times (p + 1)$ random row vector with Y one-dimensional and with $(X, Y) \sim N_{(p+1)}\left(\mu = (\mu_X, \mu_Y), \Sigma = \begin{bmatrix} \Sigma_{XX} & \Sigma_{XY} \\ \Sigma_{YX} & \sigma_Y^2 \end{bmatrix}\right)$, where Σ is nonsingular, then

$$X \sim N_p(\mu_X, \Sigma_{XX}); Y \sim N(\mu_Y, \sigma_Y^2)$$

and

$$Y|(X = x) \sim N(\mu_Y + (x - \mu_X)\Sigma_{XX}^{-1}\Sigma_{XY}, \sigma_Y^2(1 - \gamma^2))$$

where $\gamma^2 = \frac{\Sigma_{YX}\Sigma_{XX}^{-1}\Sigma_{XY}}{\sigma_Y^2}$; $\gamma = +\sqrt{\gamma^2}$.

- (R9) If $Y \sim N_n(\mu, \Sigma)$, then $\text{Cov}(Y, Y^T A Y) = 2\Sigma A \mu$ [26, Thm 5.2d].
- (R10) Let Z_1, \dots, Z_n be IID $p \times 1$ random vectors with $Z_i \sim N_p(\mu, \Sigma)$, and let

$$\bar{Z} = \frac{1}{n} \sum_{i=1}^n Z_i; S = \frac{1}{n-1} \sum_{i=1}^n (Z_i - \bar{Z})(Z_i - \bar{Z})^T.$$

Then

- (i) \bar{Z} and S are independent;

- (ii) $\bar{Z} \sim N_p(\mu, \frac{1}{n}\Sigma)$;
- (iii) $(n-1)S \sim \mathcal{W}_p(n-1, \Sigma)$; and
- (iv) $[(n-1)S]^{-1} \sim \mathcal{W}_p^{-1}(n-1, \Sigma^{-1})$.

Note that if we let Z be the $n \times p$ matrix with the i th row being Z_i^T , then

$$\bar{Z} = \frac{1}{n} \mathbf{1}_n^T Z \text{ and } S = \frac{1}{n-1} Z^T [I_n - \frac{1}{n} J_n] Z$$

where $\mathbf{1}_n$ is an $n \times 1$ column vector of 1s, I_n is the $n \times n$ identity matrix, and $J_n = \mathbf{1}_n \mathbf{1}_n^T$ is the $n \times n$ matrix of 1s. In the rest of the proof, we let

$$C_n \equiv I_n - \frac{1}{n} J_n.$$

Next, for the sample data $(X_i, Y_i), i = 1, \dots, n$, let $Y = (Y_1, Y_2, \dots, Y_n)^T$ and X be the $n \times p$ matrix with its i th row being X_i . The associated first- and second-order sample moments are:

$$\begin{aligned} \bar{X} &= \frac{1}{n} \mathbf{1}_n^T X; \quad \bar{Y} = \frac{1}{n} \mathbf{1}_n^T Y; \\ S_{XX} &= \frac{1}{n-1} X^T C_n X; \quad S_{XY} = \frac{1}{n-1} X^T C_n Y; \quad S_Y^2 = \frac{1}{n-1} Y^T C_n Y. \end{aligned}$$

Observe that C_n is symmetric and idempotent with rank $n-1$.

Since we are sampling from a multivariate normal distribution, by (R10(i)), it follows that (\bar{X}, \bar{Y}) and (S_{XX}, S_{XY}, S_Y^2) are independent. Define the $n \times p$ matrix V via $V = C_n X$. Then it is easily seen that $S_{XX} = \frac{1}{n-1} V^T V$; $S_{XY} = \frac{1}{n-1} V^T Y$. Therefore, we have

$$U_1 \equiv (S_{XX})^{-1} S_{XY} = (V^T V)^{-1} V^T Y.$$

On the other hand,

$$\frac{1}{\hat{\gamma}^2} = \frac{S_Y^2}{S_{YX} S_{XX}^{-1} S_{XY}} = 1 + \frac{U_2}{U_3}$$

where

$$U_2 = Y^T [C_n - P_V] Y; \quad U_3 = Y^T P_V Y;$$

where $P_V = V(V^T V)^{-1} V^T$ is an $n \times n$ symmetric and idempotent matrix of rank p . Also, note that $C_n - P_V$ is symmetric and idempotent with rank $n-1-p$. Letting

$$T = \sqrt{1 + \frac{U_2}{U_3}} U_1$$

the estimated MALP could be written as

$$\hat{Y}^*(x_0) = \bar{Y} + (x_0 - \bar{X})T.$$

Furthermore, since T is a function of (S_{XX}, S_{XY}, S_Y^2) , then T is independent of (\bar{X}, \bar{Y}) .

Using the iterated expectation and variance rules, and first conditioning on T , we obtain

$$\begin{aligned} \mathbb{E}[\hat{Y}^*(x_0)] &= \mathbb{E}(\mathbb{E}[\bar{Y} + (x_0 - \bar{X})T|T]) = \mu_Y + (x_0 - \mu_X)\mathbb{E}(T); \\ \text{Var}[\hat{Y}^*(x_0)] &= \text{Var}[\mathbb{E}[\bar{Y} + (x_0 - \bar{X})T|T]] + \mathbb{E}[\text{Var}[\bar{Y} + (x_0 - \bar{X})T|T]] \\ &= \text{Var}[\mu_Y + (x_0 - \mu_X)T] + \mathbb{E}\left[\frac{\sigma_Y^2}{n} + T^T \frac{\Sigma_{XX}}{n} T - 2 \frac{\Sigma_{YX}}{n} T\right] \\ &= (x_0 - \mu_X)\text{Cov}(T)(x_0 - \mu_X)^T + \frac{1}{n} [\sigma_Y^2 + \text{tr}(\Sigma_{XX}\mathbb{E}(TT^T)) - 2\Sigma_{YX}\mathbb{E}(T)] \end{aligned}$$

where tr is the trace of a matrix. Since $\mathbb{E}(TT^T) = \text{Cov}(T) + \mathbb{E}(T)\mathbb{E}(T)^T$, then

$$\begin{aligned} \text{Var}[\hat{Y}^*(x_0)] &= (x_0 - \mu_X)\text{Cov}(T)(x_0 - \mu_X)^T + \\ &\quad \frac{1}{n} [\sigma_Y^2 + \text{tr}(\Sigma_{XX}\text{Cov}(T)) + \text{tr}(\Sigma_{XX}\mathbb{E}(T)\mathbb{E}(T)^T) - 2\Sigma_{YX}\mathbb{E}(T)]. \end{aligned}$$

As such, to find the mean and variance of $\hat{Y}^*(x_0)$, we need to find $\mathbb{E}(T)$ and $\text{Cov}(T)$, then to plug-in their expressions in the expressions for $\mathbb{E}[\hat{Y}^*(x_0)]$ and $\text{Var}[\hat{Y}^*(x_0)]$.

To obtain expressions for $\mathbb{E}(T)$ and $\text{Cov}(T)$, or approximate expressions since T is a non-linear function of $U = (U_1, U_2, U_3)$, we will first obtain the means, variances, and covariances of U . By (R8), we have the distributional result that

$$Y|(X = x) \sim N_n(1_n\mu_Y + (x - 1_n \otimes \mu_X)\Sigma_{XX}^{-1}\Sigma_{XY}, \sigma_Y^2(1 - \gamma^2)I_n).$$

Recall the expressions $U_1 = (V^T V)^{-1}V^T Y$, $U_2 = Y^T(C_n - P_V)Y$, and $U_3 = Y^T P_V Y$, where $V = C_n X$, $C_n = I_n - J_n/n$, and $P_V = V(V^T V)^{-1}V^T$. We observe the following identities:

- (i) $C_n 1_n = 0$, $V^T 1_n = 0$, and $P_V 1_n = 0$
- (ii) $P_V V = P_V X = V$
- (iii) $P_V C_n = P_V$
- (iv) $(V^T V)^{-1}V^T(C_n - P_V) = 0$
- (v) $(V^T V)^{-1}V^T P_V = (V^T V)^{-1}V^T$
- (vi) $(C_n - P_V)P_V = 0$

It therefore follow from (R6) and (R7) that, given X , U_1 and U_2 are independent; U_2 and U_3 are independent; but U_1 and U_3 are not independent. From these results, we have $\text{Cov}(U_1, U_2|X) = 0$

and $\text{Cov}(U_2, U_3|X) = 0$. From (R5), noting that the ranks of $(C_n - P_V)$ and P_V are $(n - 1 - p)$ and p , respectively, coupled with the identities above, the following distributional results follow:

$$\begin{aligned} U_1|X &\sim N_p(\Sigma_{\text{XX}}^{-1}\Sigma_{\text{XY}}, \sigma_Y^2(1 - \gamma^2)(V^T V)^{-1}); \\ U_2|X &\sim \sigma_Y^2(1 - \gamma^2)\chi_{n-1-p}^2(0); \\ U_3|X &\sim \sigma_Y^2(1 - \gamma^2)\chi_p^2\left(\lambda = \frac{1}{2} \frac{\Sigma_{\text{YX}}\Sigma_{\text{XX}}^{-1}(V^T V)\Sigma_{\text{XX}}^{-1}\Sigma_{\text{XY}}}{\sigma_Y^2(1 - \gamma^2)}\right). \end{aligned}$$

To somewhat simplify the notation, letting $Z = V\Sigma_{\text{XX}}^{-1}\Sigma_{\text{XY}}$, then

$$U_3|X \sim \sigma_Y^2(1 - \gamma^2)\chi_p^2\left(\lambda = \frac{1}{2} \frac{Z^T Z}{\sigma_Y^2(1 - \gamma^2)}\right).$$

From these, we obtain the conditional means and variances using (R2) and properties of the multivariate normal distribution:

$$\begin{aligned} \text{E}(U_1|X) &= \Sigma_{\text{XX}}^{-1}\Sigma_{\text{XY}}; \quad \text{Cov}(U_1|X) = \sigma_Y^2(1 - \gamma^2)(V^T V)^{-1}; \\ \text{E}(U_2|X) &= \sigma_Y^2(1 - \gamma^2)(n - 1 - p); \quad \text{Var}(U_2|X) = [\sigma_Y^2(1 - \gamma^2)]^2 2(n - 1 - p); \\ \text{E}(U_3|X) &= \sigma_Y^2(1 - \gamma^2) \left[p + \frac{Z^T Z}{\sigma_Y^2(1 - \gamma^2)} \right]; \quad \text{Var}(U_3|X) = [\sigma_Y^2(1 - \gamma^2)]^2 \left[2p + 4 \frac{Z^T Z}{\sigma_Y^2(1 - \gamma^2)} \right]. \end{aligned}$$

In the expressions above, we see the occurrence of $(V^T V)^{-1}$ and $Z^T Z$. Since $V^T V = (n - 1)S_{\text{XX}}$, then by results (R10 (iii) and (iv)), it follows that $V^T V \sim \mathcal{W}_p(n - 1, \Sigma_{\text{XX}})$, hence $(V^T V)^{-1} \sim \mathcal{W}_p^{-1}(n - 1, \Sigma_{\text{XX}}^{-1})$. Consequently, by result (R4),

$$\text{E}[(V^T V)^{-1}] = \frac{\Sigma_{\text{XX}}^{-1}}{n - p - 2}.$$

On the other hand, recall that $Z = V\Sigma_{\text{XX}}^{-1}\Sigma_{\text{XY}}$, which is an $n \times 1$ vector. The i th element of Z is $Z_i = V_i\Sigma_{\text{XX}}^{-1}\Sigma_{\text{XY}}$. Since $V = C_n X = (I_n - J_n/n)X$, the i th component of V is

$$V_i = X_i - \bar{X} = \left(1 - \frac{1}{n}\right) X_i - \frac{1}{n} \sum_{j \neq i} X_j.$$

Consequently, it follows that

$$\text{E}(V_i) = 0 \text{ and } \text{Cov}(V_i, V_j) = \left(\delta_{ij} - \frac{1}{n}\right) \Sigma_{\text{XX}}$$

where $\delta_{ij} = I\{i = j\}$. It follows that $\text{E}(Z_i) = 0$ and

$$\text{Cov}(Z_i, Z_j) = \left(\delta_{ij} - \frac{1}{n}\right) \Sigma_{\text{YX}}\Sigma_{\text{XX}}^{-1}\Sigma_{\text{XY}} = \left(\delta_{ij} - \frac{1}{n}\right) \sigma_Y^2 \gamma^2,$$

or, in vector form,

$$Z \sim N_n(0, C_n \sigma_Y^2 \gamma^2).$$

Since C_n is symmetric idempotent with rank $n - 1$, it follows from (R5) that

$$Z^T Z \sim (\sigma_Y^2 \gamma^2) \chi_{n-1}^2(0)$$

so that $E(Z^T Z) = (n - 1) \sigma_Y^2 \gamma^2$ and $\text{Var}(Z^T Z) = 2(n - 1)(\sigma_Y^2 \gamma^2)^2$.

Using these results and employing the iterated expectation and variance/covariance rules, and upon simplifying results, especially for $\text{Var}(U_3)$, we obtain the following unconditional means, variances, and covariances:

$$\begin{aligned} E(U_1) &= \Sigma_{\mathbf{X}\mathbf{X}}^{-1} \Sigma_{\mathbf{X}\mathbf{Y}}; & \text{Cov}(U_1) &= \sigma_Y^2 (1 - \gamma^2) \frac{\Sigma_{\mathbf{X}\mathbf{X}}^{-1}}{n - p - 2}; \\ E(U_2) &= \sigma_Y^2 (1 - \gamma^2) (n - 1 - p); & \text{Var}(U_2) &= [\sigma_Y^2 (1 - \gamma^2)]^2 2(n - 1 - p); \\ E(U_3) &= \sigma_Y^2 (1 - \gamma^2) \left[p + (n - 1) \left(\frac{\gamma^2}{1 - \gamma^2} \right) \right]; \\ \text{Var}(U_3) &= 2 [\sigma_Y^2 (1 - \gamma^2)]^2 \left[p + (n - 1) \left(\frac{\gamma^2}{1 - \gamma^2} \right) \left(\frac{2 - \gamma^2}{1 - \gamma^2} \right) \right]. \end{aligned}$$

There is one more result that we need, which is $\text{Cov}(U_1, U_3)$, since we recall that U_1 and U_3 are not independent. Using (R9), we have

$$\begin{aligned} \text{Cov}(U_1, U_3 | X) &= \text{Cov}((V^T V)^{-1} V^T Y, Y^T P_V Y | X) \\ &= (V^T V)^{-1} V^T \text{Cov}(Y, Y^T P_V Y | X) = (V^T V)^{-1} V^T 2\sigma_Y^2 (1 - \gamma^2) V \Sigma_{\mathbf{X}\mathbf{X}}^{-1} \Sigma_{\mathbf{X}\mathbf{Y}}. \end{aligned}$$

By the iterated covariance rule,

$$\begin{aligned} \text{Cov}(U_1, U_3) &= E[\text{Cov}(U_1, U_3 | X)] + \text{Cov}[E(U_1 | X), E(U_3 | X)] \\ &= E[2\sigma_Y^2 (1 - \gamma^2) \Sigma_{\mathbf{X}\mathbf{X}}^{-1} \Sigma_{\mathbf{X}\mathbf{Y}}] + \text{Cov}[\Sigma_{\mathbf{X}\mathbf{X}}^{-1} \Sigma_{\mathbf{X}\mathbf{Y}}, E(U_3 | X)] = 2\sigma_Y^2 (1 - \gamma^2) \Sigma_{\mathbf{X}\mathbf{X}}^{-1} \Sigma_{\mathbf{X}\mathbf{Y}}. \end{aligned}$$

Recall that $\text{Cov}(U_1, U_2 | X) = 0$ and $\text{Cov}(U_2, U_3 | X) = 0$, so since $E(U_1 | X)$ and $E(U_2 | X)$ are constants in X , then it follows by the iterated covariance rule that $\text{Cov}(U_1, U_2) = 0$ and $\text{Cov}(U_2, U_3) = 0$.

We are now in a position to obtain approximations to $E(T)$ and $\text{Cov}(T)$. Such approximations will be obtained through a first-order Taylor expansion of $T = g(U_1, U_2, U_3)$ where

$$T = g(U_1, U_2, U_3) = \sqrt{1 + \frac{U_2}{U_3}} U_1.$$

Taking the components of the gradient of g , we have:

$$\nabla_{u_1^t} g(u_1, u_2, u_3) = \sqrt{1 + \frac{u_2}{u_3}} I_p;$$

$$\begin{aligned}\nabla_{u_2}g(u_1, u_2, u_3) &= \frac{1}{2\sqrt{1+\frac{u_2}{u_3}}}\frac{u_1}{u_3}; \\ \nabla_{u_3}g(u_1, u_2, u_3) &= -\frac{1}{2\sqrt{1+\frac{u_2}{u_3}}}\frac{u_1u_2}{u_3^2}.\end{aligned}$$

Since $\mathbb{E}(U_2)/\mathbb{E}(U_3) = (1 - \gamma^2)/\gamma^2 + o(1)$ as $n \rightarrow \infty$ and for fixed p , so that $\sqrt{1 + \mathbb{E}(U_2)/\mathbb{E}(U_3)} = 1/\gamma + o(1)$, and then

$$g(\mathbb{E}(U_1), \mathbb{E}(U_2), \mathbb{E}(U_3)) = \frac{1}{\gamma} \Sigma_{\mathbf{X}\mathbf{X}}^{-1} \Sigma_{\mathbf{X}\mathbf{Y}} (1 + o(1)).$$

The gradients, when evaluated at $u = \mathbb{E}(U)$, become

$$\begin{aligned}\nabla_{u_1^t}g(\mathbb{E}(U)) &= \frac{1}{\gamma} I_p (1 + o(1)); \\ \nabla_{u_2}g(\mathbb{E}(U)) &= \frac{1}{n} \frac{1}{2\sigma_Y^2 \gamma} \Sigma_{\mathbf{X}\mathbf{X}}^{-1} \Sigma_{\mathbf{X}\mathbf{Y}} (1 + o(1)); \\ \nabla_{u_3}g(\mathbb{E}(U)) &= -\frac{1}{n} \frac{(1 - \gamma^2)}{2\sigma_Y^2 \gamma^3} \Sigma_{\mathbf{X}\mathbf{X}}^{-1} \Sigma_{\mathbf{X}\mathbf{Y}} (1 + o(1)).\end{aligned}$$

For large n , the first-order Taylor approximation of T is therefore

$$\begin{aligned}T &= g(U_1, U_2, U_3) \approx \frac{1}{\gamma} \Sigma_{\mathbf{X}\mathbf{X}}^{-1} \Sigma_{\mathbf{X}\mathbf{Y}} + \frac{1}{\gamma} I_p (U_1 - \mathbb{E}(U_1)) + \\ &\quad \frac{1}{n} \frac{1}{2\sigma_Y^2 \gamma} \Sigma_{\mathbf{X}\mathbf{X}}^{-1} \Sigma_{\mathbf{X}\mathbf{Y}} (U_2 - \mathbb{E}(U_2)) - \frac{1}{n} \frac{(1 - \gamma^2)}{2\sigma_Y^2 \gamma^3} \Sigma_{\mathbf{X}\mathbf{X}}^{-1} \Sigma_{\mathbf{X}\mathbf{Y}} (U_3 - \mathbb{E}(U_3)).\end{aligned}$$

Also, since our interest is when n is large, observe that

$$\begin{aligned}\text{Cov}(U_1) &= \frac{1}{n} \sigma_Y^2 (1 - \gamma^2) \Sigma_{\mathbf{X}\mathbf{X}}^{-1} (1 + o(1)); \\ \text{Var}(U_2) &= 2n [\sigma_Y^2 (1 - \gamma^2)]^2 (1 + o(1)); \\ \text{Var}(U_3) &= 2n [\sigma_Y^2 (1 - \gamma^2)]^2 \left(\frac{\gamma^2}{1 - \gamma^2} \right) \left(\frac{2 - \gamma^2}{1 - \gamma^2} \right) (1 + o(1)); \\ \text{Cov}(U_1, U_3) &= 2\sigma_Y^2 (1 - \gamma^2) \Sigma_{\mathbf{X}\mathbf{X}}^{-1} \Sigma_{\mathbf{X}\mathbf{Y}}.\end{aligned}$$

We therefore have the approximations for $\mathbb{E}(T)$ and $\text{Cov}(T)$ given by:

$$\mathbb{E}(T) \approx \frac{1}{\gamma} \Sigma_{\mathbf{X}\mathbf{X}}^{-1} \Sigma_{\mathbf{X}\mathbf{Y}}$$

and

$$\begin{aligned}\text{Cov}(T) &\approx \frac{1}{\gamma^2} I_p \left[\frac{1}{n} \sigma_Y^2 (1 - \gamma^2) \Sigma_{\mathbf{X}\mathbf{X}}^{-1} \right] I_p + \left(\frac{1}{n 2\sigma_Y^2 \gamma} \right)^2 (\Sigma_{\mathbf{X}\mathbf{X}}^{-1} \Sigma_{\mathbf{X}\mathbf{Y}})^{\otimes 2} 2n [\sigma_Y^2 (1 - \gamma^2)]^2 + \\ &\quad \left(\frac{(1 - \gamma^2)}{n 2\sigma_Y^2 \gamma^3} \right)^2 (\Sigma_{\mathbf{X}\mathbf{X}}^{-1} \Sigma_{\mathbf{X}\mathbf{Y}})^{\otimes 2} 2n [\sigma_Y^2 (1 - \gamma^2)]^2 \left(\frac{\gamma^2}{1 - \gamma^2} \right) \left(\frac{2 - \gamma^2}{1 - \gamma^2} \right) -\end{aligned}$$

$$2\frac{1}{\gamma} \left(\frac{(1-\gamma^2)}{n2\sigma_Y^2\gamma^3} \right) (\Sigma_{\mathbf{X}\mathbf{X}}^{-1}\Sigma_{\mathbf{X}\mathbf{Y}})^{\otimes 2} 2\sigma_Y^2(1-\gamma^2)$$

which when simplified reduces to

$$\text{Cov}(T) \approx \frac{1}{n} \left\{ \sigma_Y^2 \frac{(1-\gamma^2)}{\gamma^2} \Sigma_{\mathbf{X}\mathbf{X}}^{-1} - \frac{(1-\gamma^2)^2}{\gamma^4} (\Sigma_{\mathbf{X}\mathbf{X}}^{-1}\Sigma_{\mathbf{X}\mathbf{Y}})^{\otimes 2} \right\}.$$

Finally, we are able to obtain the large n approximations of $\text{E}[\hat{Y}^*(x_0)]$ and $\text{Var}[\hat{Y}^*(x_0)]$. First, we have

$$\text{E}[\hat{Y}^*(x_0)] = \mu_Y + (x_0 - \mu_X)\text{E}(T) \approx \mu_Y + (x_0 - \mu_X)\frac{1}{\gamma}\Sigma_{\mathbf{X}\mathbf{X}}^{-1}\Sigma_{\mathbf{X}\mathbf{Y}} = Y^*(x_0).$$

Next, we have

$$\begin{aligned} \text{Var}[\hat{Y}^*(x_0)] &= (x_0 - \mu_X)\text{Cov}(T)(x_0 - \mu_X)^{\text{T}} + \frac{1}{n}[\sigma_Y^2 + \text{tr}(\Sigma_{\mathbf{X}\mathbf{X}}\text{Cov}(T)) + \\ &\quad \text{tr}(\Sigma_{\mathbf{X}\mathbf{X}}\text{E}(T)^{\otimes 2}) - 2\Sigma_{\mathbf{Y}\mathbf{X}}\text{E}(T)] \\ &\approx \frac{1}{n}\sigma_Y^2\frac{(1-\gamma^2)}{\gamma^2}(x_0 - \mu_X)\Sigma_{\mathbf{X}\mathbf{X}}^{-1}(x_0 - \mu_X)^{\text{T}} - \\ &\quad \frac{1}{n}\frac{(1-\gamma^2)^2}{\gamma^4}(x_0 - \mu_X)(\Sigma_{\mathbf{X}\mathbf{X}}^{-1}\Sigma_{\mathbf{X}\mathbf{Y}}\Sigma_{\mathbf{Y}\mathbf{X}}\Sigma_{\mathbf{X}\mathbf{X}}^{-1})(x_0 - \mu_X)^{\text{T}} + \\ &\quad \frac{1}{n} \left[\sigma_Y^2 + \text{tr}(\Sigma_{\mathbf{X}\mathbf{X}}\text{Cov}(T)) + \frac{1}{\gamma^2}\text{tr}(\Sigma_{\mathbf{X}\mathbf{X}}\Sigma_{\mathbf{X}\mathbf{X}}^{-1}\Sigma_{\mathbf{X}\mathbf{Y}}\Sigma_{\mathbf{Y}\mathbf{X}}\Sigma_{\mathbf{X}\mathbf{X}}^{-1}) - 2\frac{1}{\gamma}\Sigma_{\mathbf{Y}\mathbf{X}}\Sigma_{\mathbf{X}\mathbf{X}}^{-1}\Sigma_{\mathbf{X}\mathbf{Y}} \right]. \end{aligned}$$

We examine the three main terms in the above expression. The first term is

$$\begin{aligned} &\frac{1}{n}\sigma_Y^2\frac{(1-\gamma^2)}{\gamma^2}(x_0 - \mu_X)\Sigma_{\mathbf{X}\mathbf{X}}^{-1}(x_0 - \mu_X)^{\text{T}} \\ &= \frac{1}{n}\sigma_Y^2(1-\gamma^2) \left[(x_0 - \mu_X)\frac{\Sigma_{\mathbf{X}\mathbf{X}}^{-1/2}}{\gamma} \right] \left[(x_0 - \mu_X)\frac{\Sigma_{\mathbf{X}\mathbf{X}}^{-1/2}}{\gamma} \right]^{\text{T}} \\ &= \frac{1}{n}\sigma_Y^2(1-\gamma^2) \left\| (x_0 - \mu_X)\frac{\Sigma_{\mathbf{X}\mathbf{X}}^{-1/2}}{\gamma} \right\|^2. \end{aligned}$$

Similarly, the second term becomes

$$\begin{aligned} &\frac{1}{n}\frac{(1-\gamma^2)^2}{\gamma^4}(x_0 - \mu_X)(\Sigma_{\mathbf{X}\mathbf{X}}^{-1}\Sigma_{\mathbf{X}\mathbf{Y}}\Sigma_{\mathbf{Y}\mathbf{X}}\Sigma_{\mathbf{X}\mathbf{X}}^{-1})(x_0 - \mu_X)^{\text{T}} \\ &= \frac{1}{n}\sigma_Y^2(1-\gamma^2)\frac{(1-\gamma^2)}{\gamma^2} \left[(x_0 - \mu_X)\frac{\Sigma_{\mathbf{X}\mathbf{X}}^{-1}\Sigma_{\mathbf{X}\mathbf{Y}}}{\gamma\sigma_Y} \right] \left[(x_0 - \mu_X)\frac{\Sigma_{\mathbf{X}\mathbf{X}}^{-1}\Sigma_{\mathbf{X}\mathbf{Y}}}{\gamma\sigma_Y} \right]^{\text{T}} \\ &= \frac{1}{n}\sigma_Y^2(1-\gamma^2)\frac{(1-\gamma^2)}{\gamma^2} \left\| (x_0 - \mu_X)\frac{\Sigma_{\mathbf{X}\mathbf{X}}^{-1}\Sigma_{\mathbf{X}\mathbf{Y}}}{\gamma\sigma_Y} \right\|^2. \end{aligned}$$

Next, recall that $\sigma_Y^2\gamma^2 = \Sigma_{\mathbf{Y}\mathbf{X}}\Sigma_{\mathbf{X}\mathbf{X}}^{-1}\Sigma_{\mathbf{X}\mathbf{Y}}$. Therefore, $\text{tr}(\Sigma_{\mathbf{X}\mathbf{X}}\Sigma_{\mathbf{X}\mathbf{X}}^{-1}\Sigma_{\mathbf{X}\mathbf{Y}}\Sigma_{\mathbf{Y}\mathbf{X}}\Sigma_{\mathbf{X}\mathbf{X}}^{-1}) = \sigma_Y^2\gamma^2$. Also, since

$\text{Cov}(T) = \frac{1}{n}O(1)$, then $\frac{1}{n}\text{tr}(\Sigma_{\mathbf{X}\mathbf{X}}\text{Cov}(T)) = \frac{1}{n^2}O(1) = \frac{1}{n}o(1)$. Thus, the third term becomes

$$\begin{aligned} & \frac{1}{n} \left[\sigma_Y^2 + \text{tr}(\Sigma_{\mathbf{X}\mathbf{X}}\text{Cov}(T)) + \frac{1}{\gamma^2} \text{tr}(\Sigma_{\mathbf{X}\mathbf{X}}\Sigma_{\mathbf{X}\mathbf{X}}^{-1}\Sigma_{\mathbf{X}\mathbf{Y}}\Sigma_{\mathbf{Y}\mathbf{X}}\Sigma_{\mathbf{X}\mathbf{X}}^{-1}) - 2\frac{1}{\gamma}\Sigma_{\mathbf{Y}\mathbf{X}}\Sigma_{\mathbf{X}\mathbf{X}}^{-1}\Sigma_{\mathbf{X}\mathbf{Y}} \right] \\ &= \frac{1}{n} \left[\sigma_Y^2 + \frac{1}{\gamma^2}\sigma_Y^2\gamma^2 - \frac{2}{\gamma}\sigma_Y^2\gamma^2 + o(1) \right] = \frac{1}{n}\sigma_Y^2(1 - \gamma^2) \left[\frac{2}{1+\gamma} + o(1) \right]. \end{aligned}$$

Combining these expressions for the three terms, we obtain

$$\begin{aligned} \text{Var}[\hat{Y}^*(x_0)] &\approx \frac{1}{n}\sigma_Y^2(1 - \gamma^2) \times \\ &\left[\frac{2}{1 + \gamma} + \left\| (x_0 - \mu_{\mathbf{X}}) \frac{\Sigma_{\mathbf{X}\mathbf{X}}^{-1/2}}{\gamma} \right\|^2 - \frac{(1 - \gamma^2)}{\gamma^2} \left\| (x_0 - \mu_{\mathbf{X}}) \frac{\Sigma_{\mathbf{X}\mathbf{X}}^{-1}\Sigma_{\mathbf{X}\mathbf{Y}}}{\gamma\sigma_{\mathbf{Y}}} \right\|^2 \right]. \end{aligned}$$

When $p = 1$, this straight-forwardly and nicely simplifies to

$$\begin{aligned} \text{Var}[\hat{Y}^*(x_0)] &\approx \frac{1}{n}\sigma_Y^2(1 - \gamma^2) \left\{ \frac{2}{1 + \gamma} + (x_0 - \mu_{\mathbf{X}})\Sigma_{\mathbf{X}\mathbf{X}}^{-1}(x_0 - \mu_{\mathbf{X}})^{\mathbf{T}} \right\} \\ &= \frac{1}{n}\sigma_Y^2(1 - \rho^2) \left\{ \frac{2}{1 + |\rho|} + \left(\frac{x_0 - \mu_{\mathbf{X}}}{\sigma_{\mathbf{X}}} \right)^2 \right\}. \end{aligned}$$

These are the asymptotic moment results we needed to prove. Note that the asymptotic *normality* result presented in the main paper follows from the U -statistics argument. We do not need to establish this aspect of the claim in the theorem since the use of the U -statistics argument allowed us to conclude asymptotic normality under a wider class of distributions. \square

A.3 Proof of Theorem 3

When the distribution F of (X, Y) follows a multivariate normal with known parameters, then

$$Y(x_0)|(X = x_0) \sim \mathcal{N}\left(\tilde{Y}^\dagger(x_0) = \mu_Y + (x_0 - \mu_{\mathbf{X}})\Sigma_{\mathbf{X}\mathbf{X}}^{-1}\Sigma_{\mathbf{X}\mathbf{Y}}, \sigma_Y^2(1 - \rho^2)\right). \quad (31)$$

We present prediction intervals for $Y(x_0)$ under this distributional setting. We commence with the situation where the parameter values are known. Starting with the pivotal quantity

$$Q_1 = \frac{Y(x_0) - \tilde{Y}^\dagger(x_0)}{\sigma_Y\sqrt{1 - \rho^2}}$$

which, given $X = x_0$, has a standard normal distribution, the resulting $100(1 - \alpha)\%$ prediction interval for $Y(x_0)$ is

$$\left[\tilde{Y}^\dagger(x_0) \pm z_{\alpha/2}\sigma_Y\sqrt{1 - \rho^2} \right]. \quad (32)$$

For the known parameter case, we start with LSLP based on the following result:

$$\hat{Y}^\dagger(x_0) = \bar{Y} + (x_0 - \bar{X})S_{\mathbf{X}\mathbf{X}}^{-1}S_{\mathbf{X}\mathbf{Y}} \sim \mathcal{N}\left(\tilde{Y}^\dagger(x_0), \frac{1}{n}\sigma_{\text{LS}}^2(x_0)\right),$$

such that $\sigma_{\text{LS}}^2(x_0)$ is consistently estimated by

$$\hat{\sigma}_{\text{LS}}^2(x_0) = S_{\mathbf{Y}}^2(1 - \hat{\gamma}^2) \left[1 + (x_0 - \bar{X})S_{\mathbf{X}\mathbf{X}}^{-1}(x_0 - \bar{X})^\top\right]$$

with $\hat{\gamma}^2 = S_{\mathbf{Y}\mathbf{X}}S_{\mathbf{X}\mathbf{X}}^{-1}S_{\mathbf{X}\mathbf{Y}}/S_{\mathbf{Y}}^2$. We note, however, that there could be other consistent estimators of $\sigma_{\text{LS}}^2(x_0)$ (e.g., unbiased estimators) which could have better performance when the sample size is small to moderate, and they will be provided as an option in the **R** package `malp`. Note that $\text{E}\left[Y(x_0) - \hat{Y}^\dagger(x_0) \mid X = x_0\right] = \tilde{Y}^\dagger(x_0) - \tilde{Y}^\dagger(x_0) = 0$ and $\text{Var}\left[Y(x_0) - \hat{Y}^\dagger(x_0) \mid X = x_0\right] = \sigma_{\mathbf{Y}}^2(1 - \gamma^2) \left\{1 + \frac{1}{n} \left[1 + (x_0 - \mu_{\mathbf{X}})\Sigma_{\mathbf{X}\mathbf{X}}^{-1}(x_0 - \mu_{\mathbf{X}})^\top\right]\right\}$. Since the conditional variance can be consistently estimated by

$$S_{\mathbf{Y}}^2(1 - \hat{\gamma}^2) \left\{1 + \frac{1}{n} \left[1 + (x_0 - \bar{X})S_{\mathbf{X}\mathbf{X}}^{-1}(x_0 - \bar{X})^\top\right]\right\},$$

an asymptotic pivotal quantity is

$$Q_2 = \frac{Y(x_0) - \hat{Y}^\dagger(x_0)}{S_{\mathbf{Y}}\sqrt{1 - \hat{\gamma}^2}\sqrt{1 + \frac{1}{n} \left[1 + (x_0 - \bar{X})S_{\mathbf{X}\mathbf{X}}^{-1}(x_0 - \bar{X})^\top\right]}} \xrightarrow{d} \mathcal{N}(0, 1). \quad (33)$$

Using this pivotal quantity, the shortest length asymptotic $100(1 - \alpha)\%$ prediction interval for $Y(x_0)$ is

$$\left[\hat{Y}^\dagger(x_0) \pm z_{\alpha/2}S_{\mathbf{Y}}\sqrt{(1 - \hat{\gamma}^2)}\sqrt{1 + \frac{1}{n} \left[1 + (x_0 - \bar{X})S_{\mathbf{X}\mathbf{X}}^{-1}(x_0 - \bar{X})^\top\right]}\right]. \quad (34)$$

Such a prediction interval provides a quantification of the uncertainty inherent in the prediction of $Y(x_0)$ using $\hat{Y}^\dagger(x_0)$.

How about if we use the estimated MALP $\hat{Y}^\star(x_0)$ as the predicted value of $Y(x_0)$? How do we quantify the uncertainty involved in such a prediction? We may proceed analogously as in the preceding except now utilize the MALP instead of the LSLP, starting with the difference: $Y(x_0) - \hat{Y}^\star(x_0)$. First, recall the asymptotic result, conditional on $X = x_0$, in which we have

$$\hat{Y}^\star(x_0) = \bar{Y} + \frac{1}{\hat{\gamma}}(x_0 - \bar{X})S_{\mathbf{X}\mathbf{X}}^{-1}S_{\mathbf{X}\mathbf{Y}} \sim \mathcal{N}\left(\tilde{Y}^\star(x_0), \frac{1}{n}\sigma_{\text{MA}}^2(x_0)\right),$$

where σ_{MA}^2 is defined in Theorem 3.1. Thus, we have $\text{E}\left[Y(x_0) - \hat{Y}^\star(x_0) \mid X = x_0\right] = Y^\dagger(x_0) - Y^\star(x_0) = \left(1 - \frac{1}{\hat{\gamma}}\right)(x_0 - \mu_{\mathbf{X}})\Sigma_{\mathbf{X}\mathbf{X}}^{-1}\Sigma_{\mathbf{X}\mathbf{Y}} \equiv b(x_0)$. Therefore, under multivariate normality, we have

that, under $X_0 = x_0$ and for large n ,

$$Q_3 = \frac{Y(x_0) - \hat{Y}^*(x_0) - b(x_0)}{\sigma_Y \sqrt{1 - \gamma^2} \sqrt{1 + \frac{1}{n} D_{\text{MA}}^2(x_0)}} \underset{\text{approx}}{\sim} N(0, 1), \quad (35)$$

where $D_{\text{MA}}^2(x_0) = \frac{2}{1 + \gamma} + \frac{1}{\gamma^2} (x_0 - \mu_X) \Sigma_{\text{XX}}^{-1} (x_0 - \mu_X)^\top - \left[\frac{(1 - \gamma^2)}{\sigma_Y^2 \gamma^4} \right] [(x_0 - \mu_X) \Sigma_{\text{XX}}^{-1} \Sigma_{\text{XY}}]^2$. Using this as a pivotal quantity, and assuming first that we know $b(x_0)$ and $\sigma_{\text{MA}}^2(x_0)$, an approximate $100(1 - \alpha)\%$ prediction interval for $Y(x_0)$ is

$$\left[(\hat{Y}^*(x_0) + b(x_0)) \pm z_{\alpha/2} \sigma_Y \sqrt{1 - \gamma^2} \sqrt{1 + \frac{1}{n} D_{\text{MA}}^2(x_0)} \right].$$

The bias $b(x_0)$ is estimated by $\hat{b}(x_0) = \left(1 - \frac{1}{\hat{\gamma}}\right) (x_0 - \bar{X}) S_{\text{XX}}^{-1} S_{\text{XY}}$, while $\sigma_Y^2 (1 - \gamma^2) \left(1 + \frac{1}{n} D_{\text{MA}}^2(x_0)\right)$ is consistently estimated by $S_Y^2 (1 - \hat{\gamma}^2) \left[1 + \frac{1}{n} \hat{D}_{\text{MA}}^2(x_0)\right]$ with

$$\hat{D}_{\text{MA}}^2(x_0) = \frac{2}{1 + \hat{\gamma}} + \frac{1}{\hat{\gamma}^2} (x_0 - \bar{X}) S_{\text{XX}}^{-1} (x_0 - \bar{X})^\top - \left[\frac{(1 - \hat{\gamma}^2)}{S_Y^2 \hat{\gamma}^4} \right] [(x_0 - \bar{X}) S_{\text{XX}}^{-1} S_{\text{XY}}]^2.$$

Again, there could be other consistent estimators of $\sigma_{\text{MA}}^2(x_0)$ which could have better performances when the sample size is small to moderate. As such, an approximate prediction interval for $Y(x_0)$, when using the estimated MALP as the predictor, is given by

$$\left[(\hat{Y}^*(x_0) + \hat{b}(x_0)) \pm z_{\alpha/2} S_Y \sqrt{1 - \hat{\gamma}^2} \sqrt{1 + \frac{1}{n} \hat{D}_{\text{MA}}^2(x_0)} \right]. \quad (36)$$

Appendix B Additional Computer Experiments

This section complements the computational experiments reported in Section 4 of the paper. The first and second subsections provide additional results of the first computational experiment: the $p = 2$ case and the LSLP case, respectively. The third subsection investigates relationships between predictor and predictand for the MALP and the LSLP, respectively. The last subsection ascertains the asymptotic normality results of the MALP and the LSLP with respect to predicting the $Y(x_0)$ -values at fixed x_0 -values under the three different parameter sets in Table 1.

B.1 Computer Experiment 1: MALP with $p = 2$

We set $\mu = (2, 3, 1)$, and three covariance matrices were selected for Σ in order that their respective γ values are approximately 0.05, 0.5, and 0.9. The prediction points are chosen to be the intersections in the first quadrant between the contours where the squared Mahalanobis distances are

0, 1, 2, ..., 7 and a linear line crossing through μ_x with a randomly chosen positive slope equals to u_1/u_2 , where u_1 and u_2 are realizations of two independent uniform(0,1) random variables. The resulting plots are in Figures 9 and 10.

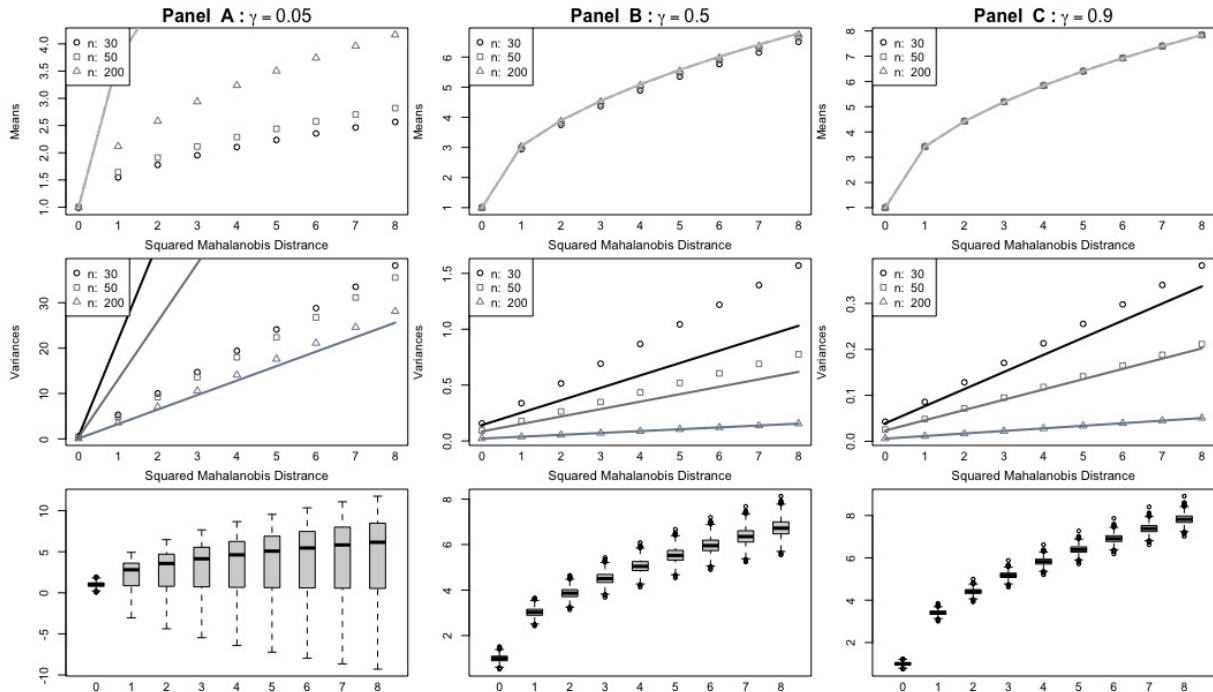


Figure 9: The approximation quality for the estimated MALP for different (γ, n) and $p = 2$: the empirical means and variances (dotted) of \hat{Y}_0^* s with their asymptotic approximations (solid curves) under the parameter sets. Also depicted are the boxplots for the case where $n = 200$.

In general, the asymptotic approximation quality when $p = 2$ is similar to that when $p = 1$, with respect to n and γ . When γ is small as in Panel A, it shows unsatisfactory approximation qualities for the means and variances for small n . However, the approximations improve as n increases. Observe also from the boxplots that when γ is small, there are more outliers on one side, which is indicative of a highly left-skewed distribution. The approximation quality improves as γ increases as seen in Panels B and C. For the means, the empirical means lie on the curve depicting the asymptotic mean function; whereas, for the variances, there are still discrepancies when the sample size is small. We surmise, and some of our (unreported) simulation results provide support to this statement, that, as p increases, larger n will be needed for the asymptotic approximations to be acceptable. In this simulation, the asymptotic variance is linear with respect to the squared Mahalanobis distance due to the choice of the set of x_0 -values. However, in general, the asymptotic variance is not linear with respect to the squared Mahalanobis distance when $p \geq 2$.

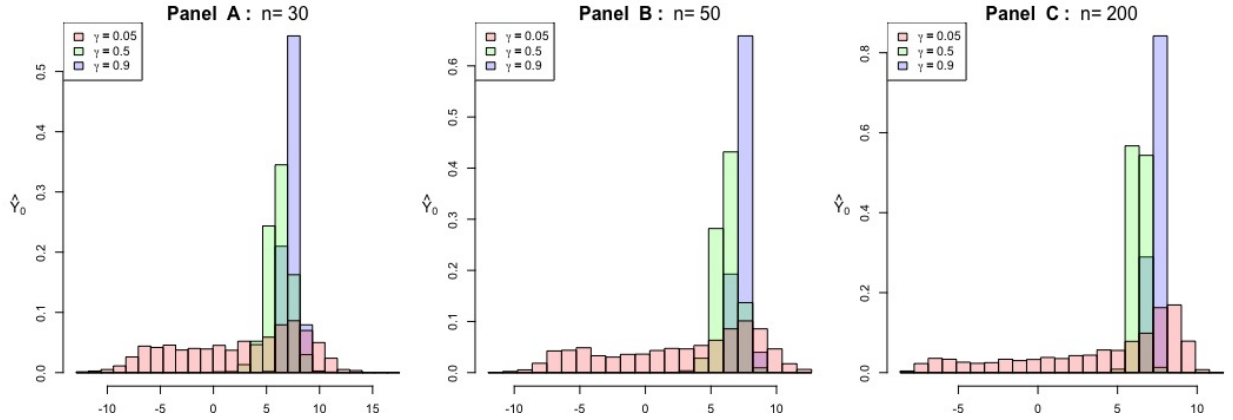


Figure 10: Empirical histograms of the estimated MALP \hat{Y}_0^* s when the squared Mahalanobis distance is 7 for different values of (γ, n) and $p = 2$ for the parameter sets based on 2000 replications.

B.2 Computer Experiment 1: LSLP with $p = 1$

The experimental results in Figure 11 show that the quality of normal approximation for the LSLP is somewhat better than that of the MALP. In particular, the LSLP consistently provides a bell-shaped distribution for $\rho = 0.05$, whereas the MALP showed unsatisfactory approximation results for the same ρ value with the sample sizes considered in the study. This can also be observed in the histograms in Figure 12, showing consistently bell-shaped distributions, compared to the bimodal distribution observed in the MALP case with $\rho = 0.05$.

B.3 Computer Experiment 3

In the third set of computer experiments, again for the specified parameter set 1 in Table 1 with ρ replaced by a value in $\{0.05, 0.5, 0.9\}$ and sample size n , for the l th replication with $l = 1, \dots, \text{MReps}$, a random sample $(X_l, Y_l) = \{(X_{li}, Y_{li}), i = 1, \dots, n\}$, as well as a single realization (X_{0l}, Y_{0l}) , is generated from the bivariate normal distribution with parameters $(\mu_X, \mu_Y, \sigma_X, \sigma_Y, \rho)$. Using this sample, the MALP and LSLP predictions of Y_{0l} , given X_{0l} , are obtained, denoted by \hat{Y}_{0l}^* and \hat{Y}_{0l}^\dagger , respectively. Figure 13 consists of scatterplots of the pairs $\{(Y_{0l}, \hat{Y}_{0l}^*), l = 1, \dots, \text{MReps}\}$ for different ρ and n values. Observe that as ρ becomes larger, the major axis of these scatterplots is the 45° line, which is to be expected from the MALP approach. For the pairs of Y_0 and \hat{Y}_0^* , the empirical versions of CCC, PCC, and MSE (more precisely, the MSPE) are utilized, and their values associated with the Y_0 and \hat{Y}_0^* are summarized in Table 5.

Note that MALP is designed to maximize the CCC between Y_0 and \hat{Y}_0^* . Therefore, the scatter plots in Figure 13 are clustered around the 45° line; whereas, the scatter plots associated with LSLP in Figure 14 are not clustered on the 45° line, especially when $|\rho|$ is small. Recall that the CCC could not exceed the PCC in absolute value, and if the parameters are known, the CCC and

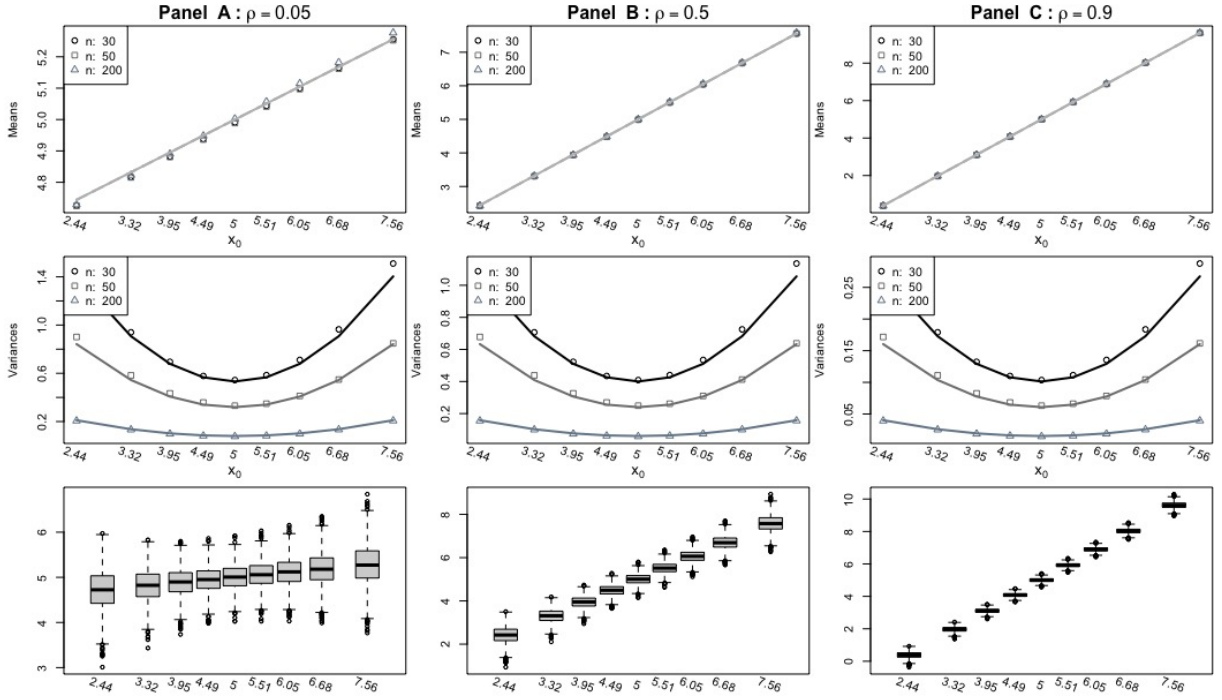


Figure 11: The approximation quality for the LSLP for different (ρ, n) : the empirical means and variances (dotted) of \hat{Y}_0^\dagger s with their asymptotic approximations (solid curves). Also depicted are the boxplots for the case when $n = 200$.

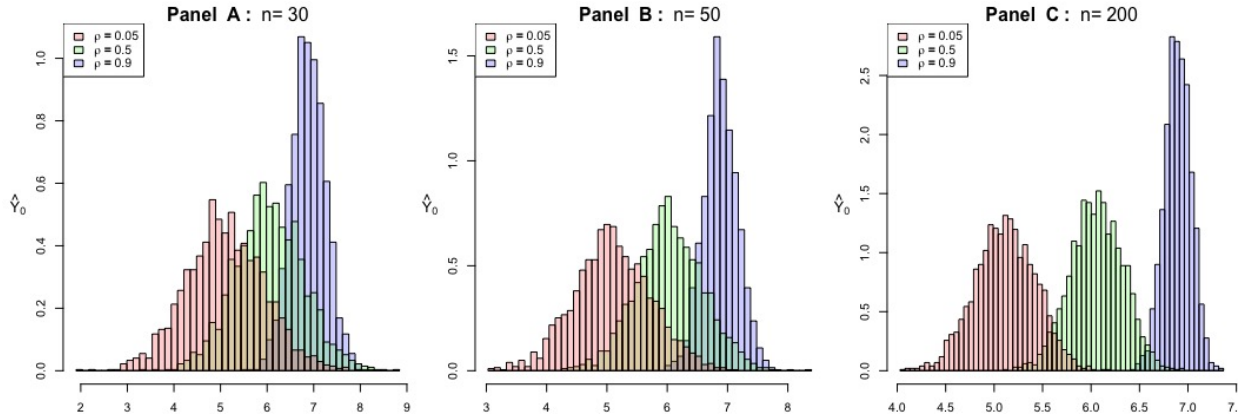


Figure 12: Empirical histograms of the estimated LSLP \hat{Y}_0^\dagger s at $x_0 = 6.05$ for different values of (ρ, n) under Parameter Set 1 based on 2000 replications.

PCC of Y_0 and \hat{Y}_0^\star are both equal to $\gamma = |\rho|$. Since we are estimating MALP based on the sample data, the CCC and PCC of the Y_0 and the predictions based on the estimated MALP need not anymore equal $|\rho|$. These two phenomena are both reflected in Table 5. In addition, compared to CCC and PCC, the MSE becomes smaller as $|\rho|$ becomes larger since clearly, the X -values will contain more information about the Y -values as $|\rho|$ increases, hence a higher predictive content.

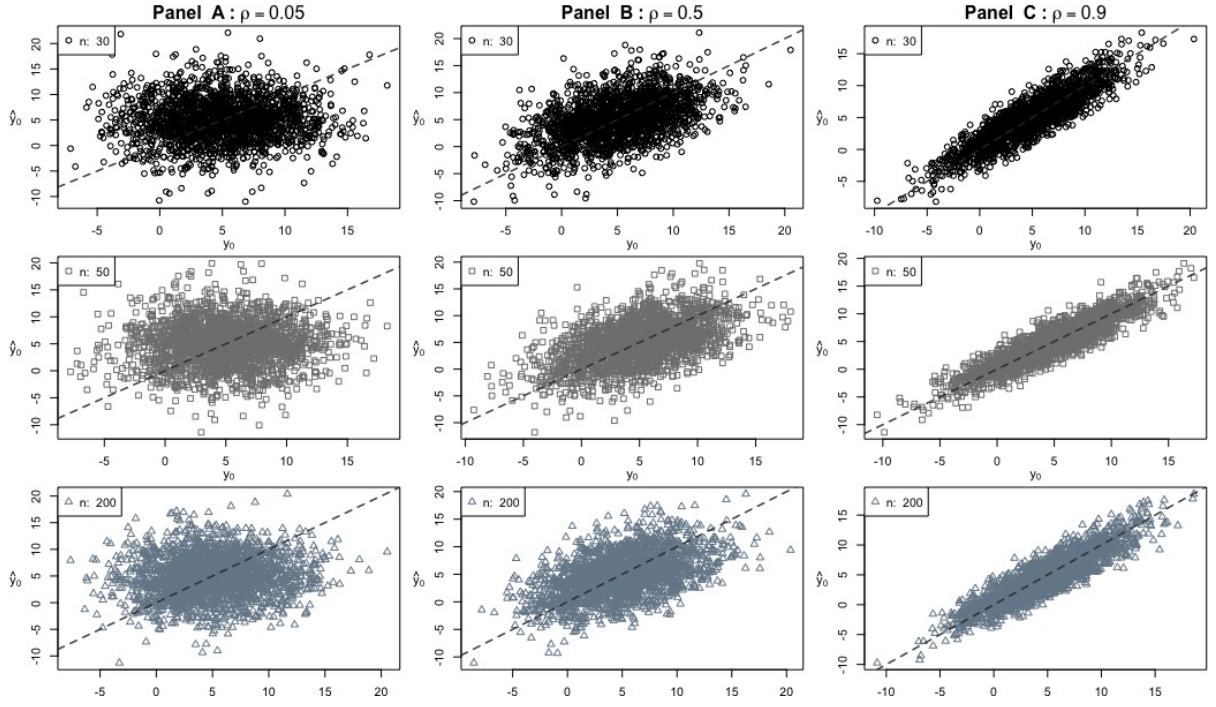


Figure 13: Scatter plots of Y_0 and \hat{Y}_0^* , together with the 45° line, for different (ρ, n) combinations.

Table 5: The performance of MALP measured by empirical PCC, CCC, and MSE from 2000 Y_0 and \hat{Y}_0^* for different (ρ, n) combinations.

ρ	$n = 30$			$n = 50$			$n = 200$		
	0.05	0.5	0.9	0.05	0.5	0.9	0.05	0.5	0.9
PCC	0.014	0.452	0.897	0.001	0.486	0.900	0.063	0.511	0.903
CCC	0.014	0.451	0.897	0.001	0.486	0.900	0.062	0.510	0.903
MSE	33.680	17.849	3.372	32.349	16.836	3.153	31.105	15.859	3.294

Compared to the scatterplots of the MALP in Figure 13, the scatterplots of the LSLP in Figure 14 are tilted from the 45° line. This tendency is more pronounced for small ρ , but the scatterplot becomes closer to the 45° line when $\rho = 0.9$.

B.4 Computer Experiment 4

In this subsection, we provide the results of another experiment to compare the functional forms of MALP and LSLP, along with the quality of the normal approximation at fixed x_0 -values or locations. The comparison was made for the three parameter sets in Table 1. We first set up the locations x_0 's to be $0, \pm 1, \pm 2$, and ± 3 standard deviations from μ_X for each parameter set. Then, we construct $\hat{Y}^*(x_0)$ and $\hat{Y}^\dagger(x_0)$ with $n = 100$ sample sizes for each x_0 point. By repeating the process, we construct the side-by-side boxplots in Figure 15 based on $\text{MReps} = 1000$ MALPs and

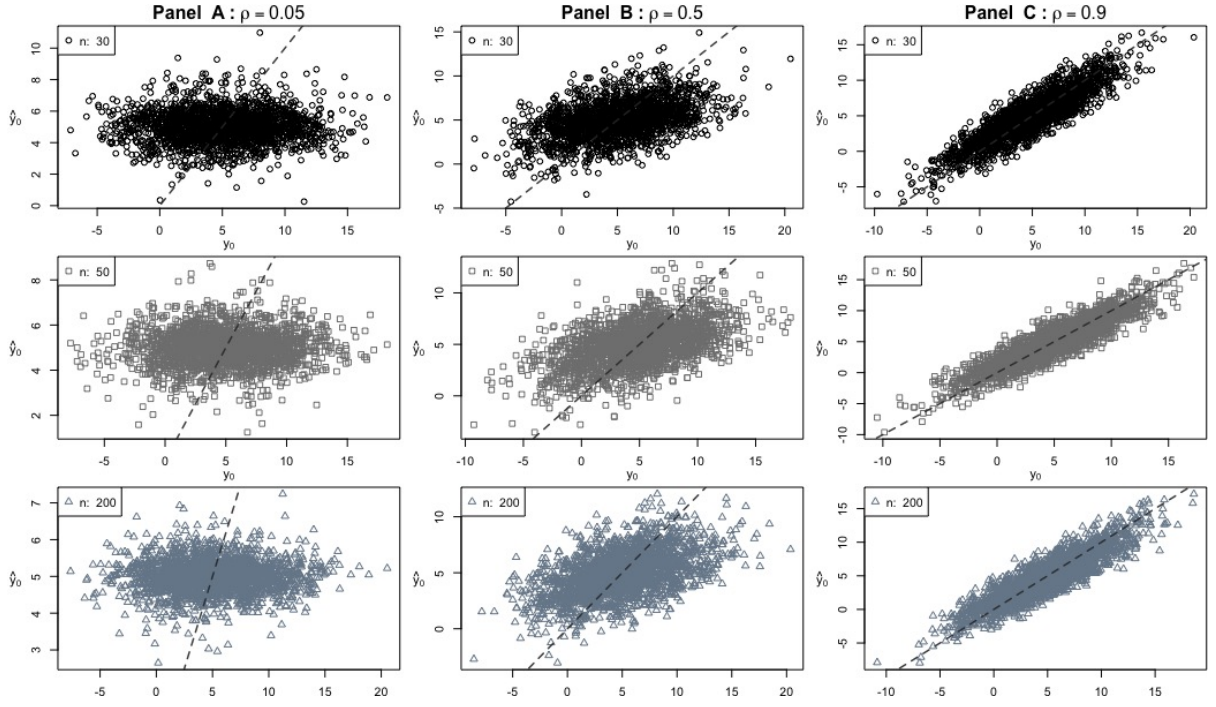


Figure 14: Scatter plots of the pairs (Y_0, \hat{Y}_0^\dagger) superimposed by 45° line for different (ρ, n) .

Table 6: The performance of the LSLP measured by empirical PCC, CCC, and MSE from 2000 Y_0 and \hat{Y}_0^\dagger for different (ρ, n) combinations.

ρ	$n = 30$			$n = 50$			$n = 200$		
	0.05	0.5	0.9	0.05	0.5	0.9	0.05	0.5	0.9
PCC	0.047	0.472	0.896	0.024	0.467	0.899	0.014	0.474	0.905
CCC	0.023	0.391	0.891	0.010	0.380	0.893	0.003	0.377	0.900
MSE	16.541	13.435	3.149	16.627	12.768	3.086	15.592	12.867	2.979

LSLPs, superimposed with the 0.005, 0.25, 0.5, 0.75, 0.995 theoretical quantiles from the normal distribution, with parameters specified in Theorem 3.1 of the main paper.

While the MALP and LSLP functions intersect at the point $x_0 = \mu_x$, the slopes of MALP are always steeper than those of LSLP, and the difference becomes larger as $|\rho|$ becomes smaller from the left plots to the right plots. The normal approximations provided by the asymptotic normality results appear good for this particular set of parameters and sample size, as could be discerned from the boxplots of the predictions from the estimated MALP and LSLP fitting well the corresponding quantiles of the approximating normal distributions. In particular, note that the sizes of boxes match well with the theoretical interquartile ranges, represented by dashed lines, from the approximating normal distributions. While the asymptotic standard errors of the MALP are greater than those of the LSLP, these differences are not so noticeable because the standard errors became quite small due to the scaling by the square root of the sample size $n = 100$.

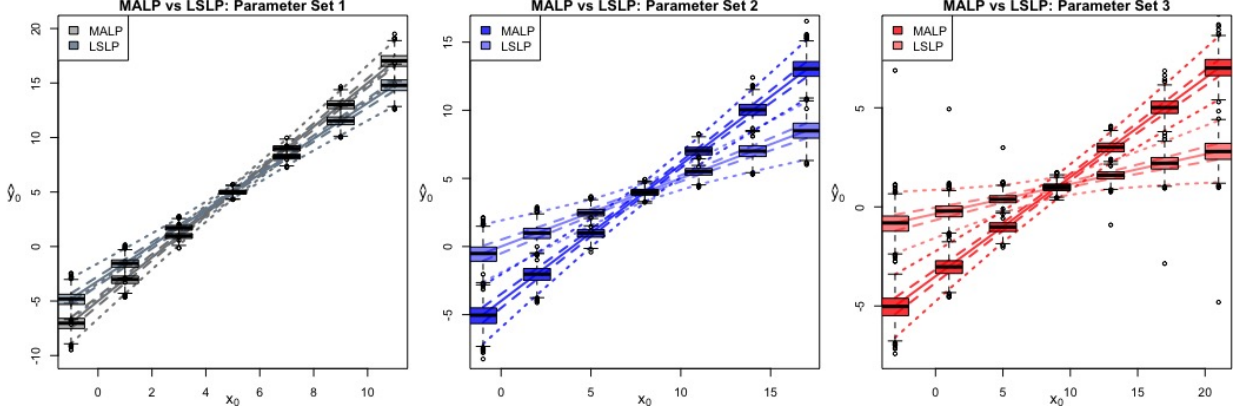


Figure 15: The comparisons between the MALP and the LSLP: the functional forms are compared at fixed points x_0 's for the three different parameter sets. The approximations to the normal distributions are also evaluated through the boxplots at each location, superimposed by the corresponding theoretical quantiles. For the three parameter sets, the associated ρ -values are 0.816, 0.5, and 0.3, from left-to-right panels.

Appendix C Forms of Confidence Intervals

We presented three approaches for approximating the standard error of $\hat{Y}^*(x_0)$, which are through the asymptotic theory via the U -Statistics, the jackknife, and the bootstrap. Approximate confidence intervals (CIs) for MALP $\tilde{Y}^*(x_0)$ could then be constructed using the approximate normality and the approximate standard errors from the three approaches mentioned. These approximate CIs for $\tilde{Y}^*(x_0)$ are provided below, where $z_{\alpha/2} = \Phi^{-1}(1 - \alpha/2)$ is the $(1 - \alpha/2)$ th quantile of the standard normal distribution, and we utilize the approximate variances provided by the asymptotic normality result, the jackknife, and the bootstrap procedures.

$$\Gamma_1[x_0, (x, y); \alpha] = \left[\hat{y}^*(x_0) \pm z_{\alpha/2} \frac{\hat{\sigma}_{MA}(x_0)}{\sqrt{n}} \right]; \quad (37)$$

$$\Gamma_2[x_0, (x, y); \alpha] = \left[\hat{y}^*(x_0) \pm z_{\alpha/2} \hat{\sigma}_{JK}(x_0) \right]; \quad (38)$$

$$\Gamma_3[x_0, (x, y); \alpha] = \left[\hat{y}^*(x_0) \pm z_{\alpha/2} \hat{\sigma}_{BS}(x_0) \right]. \quad (39)$$

For the bootstrap- t procedure, we emulate the pivot of the t -based confidence interval

$$T(x_0) = \frac{\hat{y}^*(x_0) - \tilde{y}^*(x_0)}{\hat{\sigma}_{MA}(x_0)/\sqrt{n}}$$

using the B bootstrap samples as well as the B' bootstrap sub-samples such that

$$T_b^*(x_0) = \frac{\hat{y}_b^{**}(x_0) - \hat{y}^*(x_0)}{\hat{\sigma}_{BS}^*(x_0)},$$

where $\hat{\sigma}_{BS}^*(x_0)$ is obtained by the formula in the bootstrap procedure but with the B' sub-resamples.

The estimated sampling distribution of $T(x_0)$ becomes $\hat{G}_t(z) = \frac{1}{B} \sum_{b=1}^B I\{T_b^*(x_0) \leq z\}$, called a bootstrap- t distribution. The resulting $(1 - \alpha)100\%$ bootstrap- t confidence interval is

$$\Gamma_4[x_0, (x, y); \alpha] = \left[\hat{y}^*(x_0) - \hat{G}_t^{-1}(1 - \alpha/2) \hat{\sigma}_{\text{BS}}(x_0), \hat{y}^*(x_0) - \hat{G}_t^{-1}(\alpha/2) \hat{\sigma}_{\text{BS}}(x_0) \right], \quad (40)$$

where $\hat{G}_t^{-1}(\alpha)$ is the α th-quantile of the bootstrap- t distribution and $\hat{\sigma}_{\text{BS}}(x_0)$ is from the bootstrap procedure. For the percentile approach, we utilize B bootstrap samples to obtain the same number of bootstrap replications $\hat{y}^{**}(x_0)$. The resulting bootstrap distribution is $\hat{G}_p(z) = \frac{1}{B} \sum_{b=1}^B I\{\hat{y}_b^{**}(x_0) \leq z\}$. Then, we define the $(1 - \alpha)100\%$ bootstrap percentile confidence interval as follows:

$$\Gamma_5[x_0, (x, y); \alpha] = \left[\hat{G}_p^{-1}(\alpha/2), \hat{G}_p^{-1}(1 - \alpha/2) \right], \quad (41)$$

where $\hat{G}_p^{-1}(\alpha)$ is the α th-quantile of the bootstrap distribution. Note that this approach is purely nonparametric without assuming any distributions compared to the parametric bootstrap procedure in (39). Compared to the bootstrap standard error where $B = 200$ was enough, bootstrap CI procedures generally require larger B such as 1000 or 2000. To introduce a more refined approach, we first estimate the bias-correction parameter as follows: $z_0 = \Phi^{-1}(\hat{G}(\hat{y}^*(x_0)))$. In words, z_0 is the theoretical quantile for the proportion of the bootstrap replications that are less than the observed $\hat{y}^*(x_0)$. Moreover, the acceleration parameter, a , which measures the skewness of the bootstrap distribution and can be estimated by using the jackknife replications, is

$$\hat{a} = \sum_{j=1}^n \frac{\left(\hat{y}_{(j)}^*(x_0) - \hat{y}_{(\bullet)}^*(x_0) \right)^3}{6 \left\{ \sum_{j=1}^n \left(\hat{y}_{(j)}^*(x_0) - \hat{y}_{(\bullet)}^*(x_0) \right)^2 \right\}^{3/2}}.$$

Based on these two estimated parameters, we define the bias-corrected and accelerated (BCa) bootstrap percentile CI as follows:

$$\Gamma_6[x_0, (x, y); \alpha] = \left[\hat{G}^{-1} \left\{ \Phi \left(z_0 + \frac{z_0 - z_{\alpha/2}}{1 - \hat{a}(z_0 - z_{\alpha/2})} \right) \right\}, \hat{G}^{-1} \left\{ \Phi \left(z_0 + \frac{z_0 + z_{\alpha/2}}{1 - \hat{a}(z_0 + z_{\alpha/2})} \right) \right\} \right].$$

While the BCa procedure generally provides better estimation results, its actual performance needs to be evaluated in our problem setting. In particular, the shape of the bootstrap distribution would be an important factor for comparison with the previously established asymptotic normality.

Appendix D Body Fat Data Set Description

This section provides additional information about the body fat data set [25]. The study leading to this dataset was motivated by the difficulty of obtaining the percentage of body fat, which is usually obtained through underwater weighing, so the aim is to predict the percent body fat

using easily-measured characteristics. The dataset consists of 15 variables and 252 observations. The variables are percent body fat (PBF), body density (BD), age (in years), weight (WGT, in pounds), height (HGT, in inches), and various body circumference measurements (in cm): neck (NCK), chest (CST), abdomen (ABD), hip (Hip), thigh (TGH), knee (KN), ankle (ANK), biceps (BCP), forearm (FA), and wrist (WRT). Note that the PBF variable was calculated from BD based on the equation in [28]: $PBF = 495/BD - 450$. Table 7 provides the correlation matrix for the 15 variables in the data set.

Table 7: Correlation between variables from the body fat data

	BD	PBF	Age	WGT	HGT	NCK	CST	ABD	Hip	TGH	KN	ANK	BCP	FA	WRT
BD	1.00	-0.99	-0.28	-0.59	0.10	-0.47	-0.68	-0.80	-0.61	-0.55	-0.50	-0.26	-0.49	-0.35	-0.33
PBF	-0.99	1.00	0.29	0.61	-0.09	0.49	0.70	0.81	0.63	0.56	0.51	0.27	0.49	0.36	0.35
Age	-0.28	0.29	1.00	-0.01	-0.17	0.11	0.18	0.23	-0.05	-0.20	0.02	-0.11	-0.04	-0.09	0.21
WGT	-0.59	0.61	-0.01	1.00	0.31	0.83	0.89	0.89	0.94	0.87	0.85	0.61	0.80	0.63	0.73
HGT	0.10	-0.09	-0.17	0.31	1.00	0.25	0.13	0.09	0.17	0.15	0.29	0.26	0.21	0.23	0.32
NCK	-0.47	0.49	0.11	0.83	0.25	1.00	0.78	0.75	0.73	0.70	0.67	0.48	0.73	0.62	0.74
CST	-0.68	0.70	0.18	0.89	0.13	0.78	1.00	0.92	0.83	0.73	0.72	0.48	0.73	0.58	0.66
ABD	-0.80	0.81	0.23	0.89	0.09	0.75	0.92	1.00	0.87	0.77	0.74	0.45	0.68	0.50	0.62
Hip	-0.61	0.63	-0.05	0.94	0.17	0.73	0.83	0.87	1.00	0.90	0.82	0.56	0.74	0.55	0.63
TGH	-0.55	0.56	-0.20	0.87	0.15	0.70	0.73	0.77	0.90	1.00	0.80	0.54	0.76	0.57	0.56
KN	-0.50	0.51	0.02	0.85	0.29	0.67	0.72	0.74	0.82	0.80	1.00	0.61	0.68	0.56	0.66
ANK	-0.26	0.27	-0.11	0.61	0.26	0.48	0.48	0.45	0.56	0.54	0.61	1.00	0.48	0.42	0.57
BCP	-0.49	0.49	-0.04	0.80	0.21	0.73	0.73	0.68	0.74	0.76	0.68	0.48	1.00	0.68	0.63
FA	-0.35	0.36	-0.09	0.63	0.23	0.62	0.58	0.50	0.55	0.57	0.56	0.42	0.68	1.00	0.59
WRT	-0.33	0.35	0.21	0.73	0.32	0.74	0.66	0.62	0.63	0.56	0.66	0.57	0.63	0.59	1.00

In the paper, the MALP and LSLP were obtained for increasing sizes of subsets containing the set of the best predictive variables with respect to the coefficient of determination. Subsets A, B, C, D, and E correspond, respectively, to the best subsets with 1, 2, 4, 6, and 8 variable(s). Figure 16 presents the scatter plots between predictor and predictand with respect to these subsets. Observe that the shape of the point cloud associated with the MALP predictions is more aligned with 45° line than the shape of the point cloud associated with the LSLP predictions.

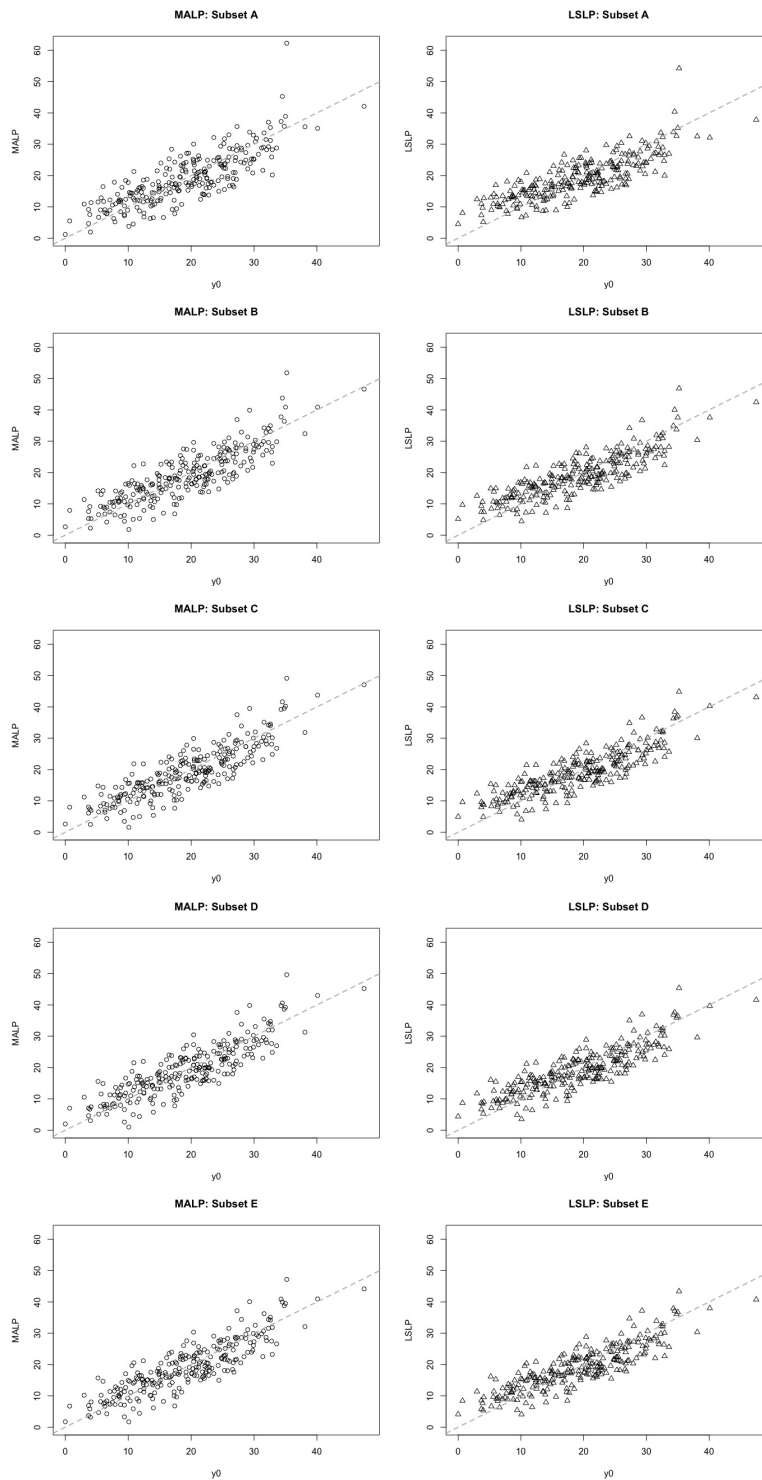


Figure 16: Scatter plots between y_0 and \hat{y}_0 , with the predicted values obtained via the MALP and LSLP, for different (increasing) subsets of predictor variables, with the dashed line being the 45° line.